

**ANKARAYILDIRIM BEYAZIT UNIVERSITY**  
**GRADUATE SCHOOL OF NATURAL AND APPLIED SCIENCES**



**INVESTIGATION AND CHARACTERIZATION OF PH EFFECT ON**  
**TiO<sub>2</sub> THIN FILM SURFACE**

**M.Sc. Thesis by**  
**Güldane ERTUĞRUL**

**Department of Materials Engineering**

**December, 2016**

**ANKARA**

**INVESTIGATION AND CHARACTERIZATION OF PH  
EFFECT ON TiO<sub>2</sub> THIN FILM SURFACE**

**A Thesis Submitted to**

**the Graduate School of Natural and Applied Sciences of Yıldırım Beyazıt  
University**

**In Partial Fulfillment of the Requirements for the Degree of Master of Science  
in Materials Engineering, Department of Materials Engineering**

**by**

**Güldane ERTUĞRUL**

**December, 2016**

**ANKARA**

## M.Sc. THESIS EXAMINATION RESULT FORM

We have read the thesis entitled “**INVESTIGATION AND CHARACTERIZATION OF PH EFFECT ON TiO<sub>2</sub> THIN FILM SURFACE**” completed by **Güldane ERTUĞRUL** under supervision of **Prof. Dr. Hasan OKUYUCU** and we certify that in our opinion it is fully adequate, in scope and in quality, as a thesis for the degree of Master of Science.

.....  
Prof. Dr. Hasan OKUYUCU

Supervisor

.....  
Prof. Dr. Hayrettin AHLATÇI

Jury member

.....  
Asist. Prof. Dr. M. Fatih ÖKTEM

Jury Member

.....  
Prof. Dr. Fatih Vehbi ÇELEBİ

Director

Graduate School of Natural and Applied Sciences

## ETHICAL DECLARATION

I have prepared this dissertation study in accordance with the Rules of Writing Thesis of Yildirim Beyazıt University of Science and Technology Institute;

- Data I have presented in the thesis, information and documents that I obtained in the framework of academic and ethical rules,
- All information, documentation, assessment and results that I presented in accordance with scientific ethics and morals,
- I have gave references all the works that I were benefited in this dissertation by appropriate reference,
- I would not make any changes in the data that I were used,
- The work presented in this dissertation I would agree that the original,

I state, in the contrary case I declare that I accept the all rights losses that may arise against me.

# INVESTIGATION AND CHARACTERIZATION OF PH EFFECT ON TiO<sub>2</sub> THIN FILM SURFACE

## ABSTRACT

Thin film solar technology is used various devices that convert the sun light into electrical energy. These applications have been crucial for human life since they supply us clean and alternative energy sources. For this application many components can be used Cu<sub>2</sub>S, CdTe, CIGS, CNTS, and TiO<sub>2</sub> etc. TiO<sub>2</sub> is one of them and preferable for this technology because of its good electrical and physical properties.

TiO<sub>2</sub> based solutions prepared completely transparent are coated on ITO glass with different Ph values, sol gel dip coating method. This coated glass annealed with same temperature and same holding time.

Previous research shows that pH factor has significant effect on the surface morphology of films. Surface area and surface roughness are pH dependent parameters that very important for light conversion efficiency.

In this study, the effect of pH on thin film surface morphology is investigated. 4 different Ph values sols are coated on ITO glass. These glasses annealed in the furnace with same temperatures and same holding time. The results are determined with several methods. Chemical properties determine by X-ray photoelectron scanning (XPS), X ray diffraction scanning (XRD) surface properties and roughness values investigated by atomic force microscopy (AFM), and ellipsometry. The XPS and XRD results show that, because of the low working temperatures there is not any change in chemical structure of TiO<sub>2</sub>. The material that we study is glass. Above 600°C chemical structure of glass can be deteriorated. We carried out our experiment below this temperature.

**Keywords:** TiO<sub>2</sub>, Thin Film, pH, surface area, surface roughness.

# TiO<sub>2</sub> İNCE FİLM YÜZEYİNE PH FAKTÖRÜNÜN ETKİSİNİN ARAŞTIRILMASI VE KARAKTERİZASYONU

## ÖZ

Bu çalışmada TiO<sub>2</sub> esaslı farklı pH değerine sahip çözeltiler hazırlanmış ve cam altlık üzerine kaplaması yapılmıştır. Kaplanan çözeltiler ısıtılarak tabii tutularak ince film oluşumu gerçekleştirilmiştir. Amaç pH etkisinin film yüzey alanına etkisini araştırmak ortalama pürüzlülük değerlerini hesaplamaktır. Bu amaçla sol gel daldırma kaplama yöntemi ile kaplaması yapılan numuneler aynı sıcaklık ve sürelerde ısıtılarak tabii tutulmuştur. Alınan sonuçlara göre artan pH ile daha pürüzlü bir film yüzeyi elde edilmesine sebep olmuştur.

**Anahtar kelimeler:** TiO<sub>2</sub>, İnce Film, pH, yüzey alanı, yüzey pürüzlülüğü.

## **ACKNOWLEDGEMENTS**

I would like to express my deep gratitude to my advisor Prof. Dr. Hasan OKUYUCU for his guidance, motivation, encouragement and criticism during my whole master education. His experience always helped me at every steps of my thesis. I will be grateful to him to the end of my life.

Besides my advisor, I would like to thank to Prof. Dr. Cihangir Duran for his helps and ideas during an experimental step of my study. I have learned many things from him.

I would also like to thank to all UNAM stuff. Especially Unam engineers of Dr. Mustafa ÜREL and Dr. Enver Kahveci for their AFM and XPS, XRD investigations. I am grateful them for their kindness and support throughout my studies.

I appreciate to my family for their endless support and courage during my whole life. Besides them my devoted and best friends Aynur İNAN, Merve TEBER, Mehmet and ESRA, I am also indebted to them.

I thank to my husband Şaban ATEŞOĞLU for his encouragement and understanding.

Finally my deepest appreciation goes to my brother Hikmet ERTUĞRUL because he always supports me.

**2016, 07 DECEMBER**

**Güldane ERTUĞRUL**

## CONTENTS

M.Sc. THESIS EXAMINATION RESULT FORM.....	ii
ETHICAL DECLARATION .....	iii
ABSTRACT.....	iv
ÖZET.....	v
ACKNOWLEDGEMENTS .....	vi
CONTENTS .....	vi
ABBREVIATION .....	ix
LIST OF TABLES .....	x
LIST OF FIGURES .....	xi
<b>CHAPTER 1 - INTRODUCTION.....</b>	<b>1</b>
1.1 TiO <sub>2</sub> and Polymorphism of TiO <sub>2</sub> .....	3
1.2 Photocatalysed reactions of TiO <sub>2</sub> .....	7
1.3 Chemical Coating Techniques.....	12
1.3.1 Chemical Vapor Deposition.....	12
1.3.2 Sol-Gel Deposition Techniques.....	13
1.3.2.1 Dip Coating Method: .....	14
1.3.2.2 Spin Coating Method .....	16
1.3.2.3 Spray Coating Method .....	17
1.3.2.4 Flow Coating Processes: .....	17
1.3.2.5 Capillary Coating:.....	18
1.3.3 Spray Pyrolysis Technique.....	19
1.4 Physical Coating Techniques .....	19
1.4.1 Sputter deposition.....	19
1.4.2 Evaporation deposition .....	21
1.5 Synthesis Reaction of TiO <sub>2</sub> Nanoparticles by Sol-Gel Method .....	23
<b>CHAPTER 2 - EXPERIMENTAL PROCEDURES.....</b>	<b>26</b>
2.1 Materials .....	26
2.1.1 Indium tin oxide .....	26
2.1.2 Sample preparation .....	28
2.1.2.1 Solution .....	28



2.1.2.2 Ph Value of Coating Solution .....	29
2.1.2.3 Drying/Firing the Coating.....	31
2.1.2.4 Samples .....	32
2.1.2.5 Etching .....	32
2.1.2.6 Process .....	33
2.1.2.7 Annealing Process.....	34
2.2 Characterizations .....	35
2.2.1 Surface Analysis.....	35
2.2.1.1 Surface Sensing.....	37
2.2.1.2 Detection Method.....	38
2.2.1.3 Imaging .....	38
2.2.2 Thickness Measurements .....	39
2.2.3 Chemical Measurements .....	41
2.2.3.1 XPS Analysis .....	41
2.2.3.2 XRD Analysis .....	45
<b>CHAPTER 3-RESULTS AND DISCUSSIONS .....</b>	<b>48</b>
3.1 Chemical Analysis.....	48
3.1.1 XPS Characterization.....	48
3.1.2 XRD Characterization .....	51
3.2 Thickness Measurements.....	52
3.2.1 SEM and Focused Ion Beam Microscopy Examinations .....	52
3.3 Surface Morphologies of Films .....	54
3.3.1 Atomic Force Microscopy (AFM) .....	54
<b>CHAPTER 4- CONCLUSION AND RECOMMENDATIONS .....</b>	<b>60</b>
4.1 Conclusion.....	60
4.2 Recommendations .....	60
<b>REFERENCES.....</b>	<b>60</b>
<b>RESUME(CV) .....</b>	<b>60</b>

## ABBREVIATION

AFM	Atomic Force Microscopy
SC	Solar Cell
TF	Thin Film
CDTE	Cadmium Telluride
CIGS	Copper Indium Gallium Di Selenide
CVD	Chemical Vapor Deposition
DSSC	Dye Sensitized Solar Cell
ECD	Electrochemical Deposition
EPMA	Electron Probe Micro Analyzer
eV	Electron volt
FIB	Focussed Ion Beam
FPD	Flat Panel Displays
ITO	Indium Tin Oxide
NT	Nanotube
PSPD	Positive-sensitive photo diode
PV	Photovoltaic
QD	Quantum Dot
Ra	Average Roughness
RMS	Root Mean Square
SC	Solar Cell
SEM	Scanning Electron Microscopy
TF	Thin Film
TiO <sub>2</sub>	Titanium dioxide
UHV	Ultra High Vacuum
UV	Ultra violet
XPS	X-ray Photoelectron Spectroscopy
XRD	X-ray Diffractometers
XRF	X-ray Fluorescence

## LIST OF TABLES

<b>Table 1.1</b> Properties of anatase and rutile .....	5
<b>Table 1.2</b> Some TiO <sub>2</sub> SC application results and their efficiency behaviour .....	9
<b>Table 2.1</b> Properties of ITO coated glass (Sigma Aldrich) .....	27
<b>Table 2.2</b> List of chemicals .....	28
<b>Table 2.3</b> Process steps.....	34
<b>Table 2.4</b> Sample list .....	35
<b>Table 2.5</b> The analysis parameters of AFM .....	39
<b>Table 2.6</b> Scanning parameters of XPS analysis.....	44
<b>Table 3.1</b> Effect of pH on surface Ra values of samples (Gwyddion-2.36.win32.pro) .....	58

## LIST OF FIGURES

<b>Figure 1.1</b> Crystal structure of anatase titanium dioxide [2].....	3
<b>Figure 1.2</b> Crystal structure of rutile titanium dioxide [2] .....	4
<b>Figure 1.3</b> Reaction boundaries of phase transitions in TiO <sub>2</sub> [6] .....	4
<b>Figure 1.4</b> Working Principle of TiO <sub>2</sub> Solar Cell [2].....	7
<b>Figure 1.5</b> Schematic illustration of photo-generation of charge carriers [6]. .....	8
<b>Figure 1.6</b> Coating steps of dip coating process (1) dipping (2) immersing (3) evaporation.....	14
<b>Figure 1.7</b> Schematic representation of dip coating process.....	15
<b>Figure 1.8</b> Schematic diagram of the stages of the spin coating process[20] .....	16
<b>Figure 1.9</b> Schematic diagram of the flow coating process[20].....	18
<b>Figure 1.10</b> Schematic representation of capillary coating [20] .....	18
<b>Figure 1.11</b> Sputtering mechanism [23].....	20
<b>Figure 2.1</b> Indium Tin Oxide Glass.....	27
<b>Figure 2.2</b> The resulting solution is totally homogenous.....	29
<b>Figure 2.3</b> The solution prepared with Titanium methoxide is fully transparent.....	29
<b>Figure 2.4</b> The solution prepared with titanium nitrate cannot be solved completely .....	29
<b>Figure 2.5</b> Desktop type Ph meter .....	30
<b>Figure 2.6</b> Solutions with different pH values .....	31
<b>Figure 2.7</b> Vertical Drying Furnaces.....	32
<b>Figure 2.8</b> Sol-Gel Dip Coating Method.....	33
<b>Figure 2.9</b> Annealing furnace.....	34
<b>Figure 2.10</b> Temperature profile applied for thermal treatment of the samples .....	35
<b>Figure 2.11</b> Working principle of AFM instrument.....	36

<b>Figure 2.12</b> Schematic representation of interaction forces versus tip distance .....	38
<b>Figure 2.13</b> Working principle of XPS .....	42
<b>Figure 2.14</b> X-ray Photoelectron Spectroscopy (UNAM) .....	44
<b>Figure 2.15</b> Schematic representation of Bragg Law .....	46
<b>Figure 2.16</b> X-Ray Diffractometer .....	47
<b>Figure 3.1</b> XPS scanning result of TiO <sub>2</sub> thin films.....	48
<b>Figure 3.2</b> XPS scanning result of TiO <sub>2</sub> thin films after Ar etching .....	49
<b>Figure 3.3</b> Binding energy peaks of TiO <sub>2</sub> and O <sub>2</sub> .....	50
<b>Figure 3.4</b> XRD analysis results of thin films.....	51
<b>Figure 3.5</b> Thickness measurements with SEM [59]. .....	53
<b>Figure 3.6</b> AFM XEI program profilometer images the samples of A1, A2, A3, and A4.....	54
<b>Figure 3.7</b> AFM images of TiO <sub>2</sub> samples with different pH. (A1, A2, A3, A4 and B1).....	56
<b>Figure 3.8</b> Average roughness versus pH.....	57
<b>Figure 3.93</b> DAFM images of samples (A1, A2, A3, A4, and B1) (Gwyddion-2.36.win32.pro).....	59

# CHAPTER 1

## INTRODUCTION

Increasing human population cause increasing energy demand and bring together some problems. The sources in our world became insufficient. For this reason alternative resources attract researchers and various devices developed to take an advantage of our natural power. Photovoltaic and solar cell technology provided us obtaining alternative energy from the sun. Solar cell technology is available for transform solar energy into electrical energy. This technique is performed to power electrical devices. In a lot of homes and workplaces SCs are used for supporting alternative energy. The importance of this technology is undeniable. In near future such an alternative devices became a must. With further development and larger admission this technology became a solution to the increasing energy demand. So, improve the efficiency of these cells have been our priority objectives [1].

Various SCs are available such as, thin film SC, polycrystalline and single crystalline silicon SC, photochemical SC etc. Thin film SC is produced by coating one or more thin layers on a substrate material. These layers which coated on a substrate also be PV material, glass, plastic or metal. Due to large scale power generation TF photovoltaics are advantageous. This technology offers us high production capacity with using less material and energy entrance in the manufacturing step process and by the deposition process this technique can be integrated module structures [2-4].

According to Green the crystalline silicon is the first generation photovoltaic technology and the second one is TFPVs. TF crystalline silicon, copper indium gallium diselenide (CIGS), amorphous silicon (a-Si), cadmium telluride (CdTe) etc. all of them are TFCS materials. “(Green, 2001).”

Typical silicon SC has less absorption coefficient than TF semiconductors and also TFSCs needs thinner layer than Si. So with this way less material used for the semiconductor layer in TFSC. Thus, the cost of semiconductor material is

decreased; more expensive semiconductors can be used in TF. “(Goetzberger&Hebling, 2000).”

The properties which given below are the reasons for the preference of TF technology.

- ✓ There are many deposition techniques for fabrication of thin film. These techniques are chemical, physical, electrochemical and plasma deposition techniques.
- ✓ According to deposition technique, process parameter and substrate material different microstructures can be obtained in TF materials.
- ✓ Different shapes, sizes, areas and various types of substrate materials are present.
- ✓ Due to easy solubility properties compatible and incompatible materials can be produced.
- ✓ With appropriate components the deactivation operation of grain surface and the boundaries is possible.
- ✓ Various kinds of arrangements can be obtained. For example, single, tandem and electronic junctions.
- ✓ Various characteristic features can be obtained with desired value.
- ✓ Surface properties can be changed to supply barrier effect for interlayer diffusion.
- ✓ For obtaining proper optical reflectance-transmission ratio surface modification can be possible.
- ✓ For fabricating SC, combination of unit and singular SC can be accessible.
- ✓ TFs are called ‘Green Processes’ apart from material and energy conversation they are environmentally benign [5].

## 1.1 TiO<sub>2</sub> and Polymorphism of TiO<sub>2</sub>

Titanium dioxide is used in this study because of its attractive properties. Among all elements TiO<sub>2</sub> is the ninth most abundant element in the earth. “(Gullichsen, 2000)”. Pure TiO<sub>2</sub> is a form of crystalline. It is situated in d block of periodic table and shows same properties as other d block elements. “(Lewis 1988).”

At atmospheric pressure condition Ti is naturally found in oxide form of titanium. Rutile, anatase and brookite terms are three polymorphs structure of TiO<sub>2</sub>. Rutile is stable and the others are metastable phase. Brookite phase is rarely studied because its synthesis is quite difficult. Besides them TiO<sub>2</sub> has five high pressure phase.

- ✓ Type of srilankite polymorph,
- ✓ Type of cubic fluorite polymorph,
- ✓ Type of pyrite polymorph
- ✓ Type of monoclinic baddeleyite polymorph,
- ✓ Type of cotunnite polymorph [6].

Rutile and anatase are two different forms of TiO<sub>2</sub> are given below [2].

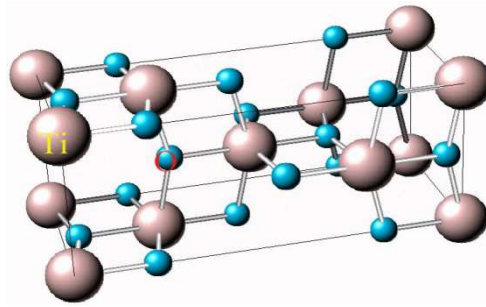


**Figure 1.1.**Crystal structure of anatase titanium dioxide [2].



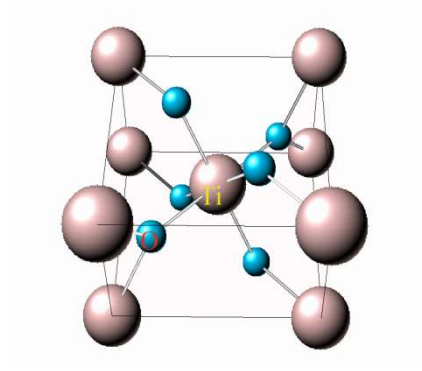


**Figure 1.2.**Crystal structure of rutile titanium dioxide [2].

A crystal structure of rutile form is more compact than anatase form. Due to this chemical structure density and refractive index values of anatase is very low and less stable than rutile ”(Gullichsen, 2000)”

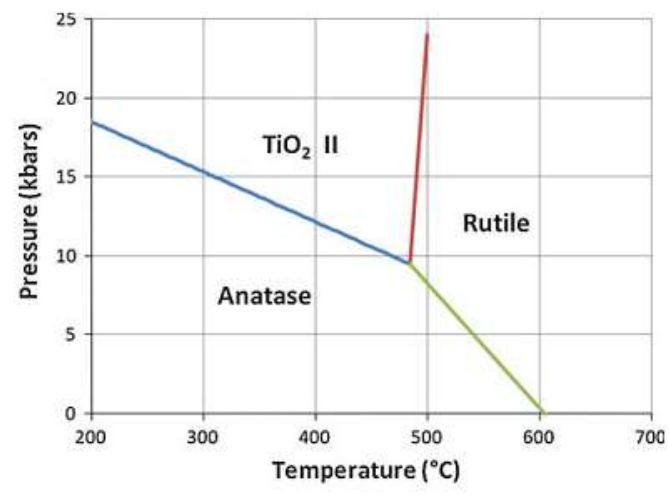


**Figure 1.3** Reaction boundaries of phase transitions in TiO<sub>2</sub> [6].

**Table 1.1** Properties of anatase and rutile [6].

Property	Anatase	Rutile
Crystal structure	Tetragonal	Tetragonal
Atoms per unit cell(Z)	4	2
Space group	$I\frac{4}{a}md$	$p4_2/mnm$
Lattice parameters(nm)	a = 0,3785 c = 0,9514	a = 0,4594 c = 0,29589
Unit cell volume(nm <sup>3</sup> )a	0,1363	0,0624
Density(kg m <sup>-3</sup> )	3894	4250
Calculated indirect band gap (eV)	3,23-3,59	3,02-3,24
(nm)	345,4-383,9	382,7-410,1
Experimental band gap (eV)	~3,2	~3,0
(nm)	~387	~413
Refractive index	2,54 , 2,49	2,79 , 2,903
Solubility in HF	Soluble	Insoluble
Solubility in H <sub>2</sub> O	Insoluble	Insoluble
Hardness (Mohs)	5,5-6	6-6,5
Bulk modulus (GPa)	183	206

Titania is also used various technological areas;

- Energy
  - ✓ Electrolysis of water to produce hydrogen
  - ✓ DSSCs
  
- Environment
  - ✓ Purification of air
  - ✓ Water treatment
  
- Built Environment
  - ✓ Self-cleaning coatings
  - ✓ Non-spotting glass
  
- Biomedicine
  - ✓ Self-sterilizing coatings [6].

As Sommeling and Späth(2008) said thatTiO<sub>2</sub> SC has the potential to reach low costs in future power technologies.

An equipment of TiO<sub>2</sub> SC needs quite low power output since this is easily obtained. Fabrication process of SC is more flexible due to the efficiency concern is less strict.

Since the fabrication process is more flexible and the costs are lower, SC technology provides to researchers alternative production. “(Sommeling&Späth 2008).”

Due to the good photocatalytic properties of TiO<sub>2</sub> it is very fine material for solar cells.

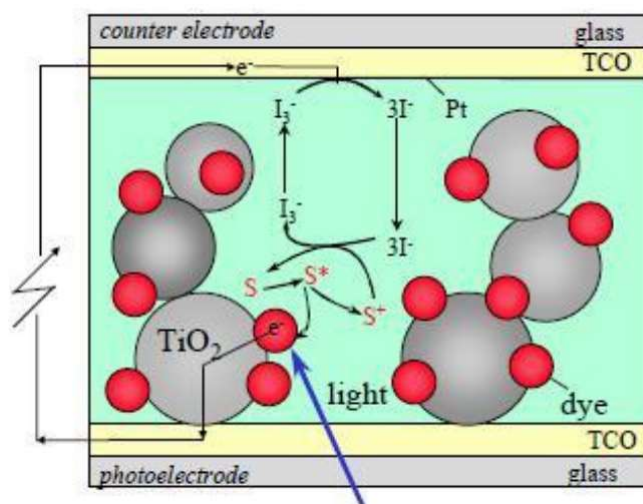


Figure 1.4 Working Principle of TiO<sub>2</sub> Solar Cell [2].

Three primary steps of the working phenomena of PV cell are given below:

- ✓ Light absorption
- ✓ Charge separation
- ✓ Charge collection

TiO<sub>2</sub> is very attractive material because of its good properties. It has convincing energy conversion efficiency values, fabrication process of it is quite easy and also low cost material. Additionally all the photocatalytic effect of TiO<sub>2</sub> is relatively high.

## 1.2 Photocatalysed reactions of TiO<sub>2</sub>

TiO<sub>2</sub> surface contains adsorbed radical groups which are come from air or water. Through these radicals photo catalysed reactions happen easily. These radicals have free unpaired electrons. When TiO<sub>2</sub> surface exposed the radiation energy these free electrons formed. Than an electron is move to conduction band from the valance band. As shown in Figure 1.5 these electrons which move from valance band to conduction band leave behind an electron hole in the conduction band. The electrons cause the reduction of electron acceptors while the holes cause an oxidation of electron donors. Following reactions are given below explained the photo generation of radicals clearly.

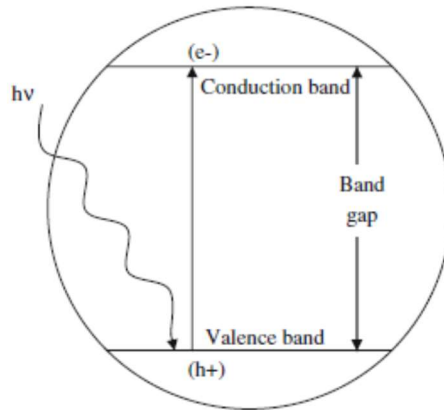
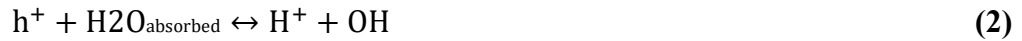


**Figure 1.5** Schematic illustration of photo-generation of charge carriers [6].



In this reactions, a point is demonstrated an unpaired electron,  $h^+$  is the electron hole of valance band and an conduction band electron is symbolized by  $e^-$ .

Positive and negative charge carriers are formed by UV radiation. They tended to recombine and one way or another semiconductor is working as a photocatalyst. Titania's photocatalytic ability is depends on its high surface area. This property affects its optical properties at the same time. Due to high surface area the electrons of which energy values are between the conduction band and valance band have higher density. These electrons are come from finalized and unsaturated bonds on the surface. Because of these sites charge separation phenomena is occurred easily. For photo-generated charge carriers, these areas are excellent trapping sites. Among all semiconductors  $\text{TiO}_2$  has rather small rate of charge recombination. There is a suggestion about this situation point out the photo generated electron-hole pair

requires min 0,1 ns life time for chemical reactions. And this situation makes TiO<sub>2</sub> quite advantageous [6].

Reactive components adsorbed by the catalyst surface, photo generated charge carriers prefer transferring to these adsorbates and forming radicals to recombining. So, it can be understood that for better and effective photo catalysation presence high density of reactive adsorbed species is essential [6].

One of the main reasons of TiO<sub>2</sub> usage in DSSC research is having high energy conversion efficiency. The table shows the efficiency result which are found by Gratzel group “(Green 2001, Grätzel 2000, Nazeeruddin et al. 1993, O'Regan&Grätzel 1991)”

**Table 1.2** Some TiO<sub>2</sub> SC application results and their efficiency behaviour. “(Halme 2002)” [2].

Semi-conductor	Dye	$\eta$ (%)	Area (cm <sup>2</sup> )	Illumination(mW/cm <sup>2</sup> )	Reference
TiO <sub>2</sub>	?	11	0,25	100 (AM1,5)	Green 2001
TiO <sub>2</sub>	Black Dye	10,4	?	100(AM1,5)	Gratzel 2000
TiO <sub>2</sub>	N3	10,0	0,3	96(AM1,5)	Nazeeruddin et al. 1993
TiO <sub>2</sub>	N719 <sup>22</sup>	9,2	1,5	? (AM1,5)	Deb et al. 1998
TiO <sub>2</sub>	RuL <sub>2</sub> ( $\mu$ -	7,1	0,5	75(AM1,5)	O'Regan&Gratzel 1991
	(CN)Ru(CN)L'' <sub>2</sub> ) <sub>2</sub>	7,9		8(AM1,5)	O'Regan&Gratzel 1991
TiO <sub>2</sub>	N3	6	1	100 (ELH LAMP)	Hagfeldt et al. 1994
		7,3		11,5(ELH LAMP)	Hagfeldt et al. 1994
TiO <sub>2</sub>	A Ru-phenantrolin derivative	6,1	0,44	100(AM1,5)	Yanagida et al. 2000
TiO <sub>2</sub>	A coumarin derivative	5,6	?	100(AM1,5)	Hara et al.2001a
TiO <sub>2</sub>	Cu-2-a-oxymesoisochlorin	2,6	0,5	100 (''white light'')	Kay&Gratzel 1993
TiO <sub>2</sub>	A natural chain- dye	0,56	0,9	100(AM1,5)	Cherepy et al. 1997

L=2,2'bipyridyl-4,4'-dicarboxylic

L''=2,2'bipyridine

For achieving high energy conversion efficiency in the DSSCs a dye is very important. The dye must be an efficient charge transfer sensitizer and the table shows also the most favored dye is improved by the Gratzel group.

According to Gratzel as an electron acceptor to support a molecular or DT sensitizer in DSSC technology  $\text{TiO}_2$  is the most major nanocrystalline semiconductor oxide electrode [7].

Zhu et al. in DSSC technology new researches shows that  $\text{TiO}_2$  surface morphology is fairly important for cell efficiency and light scattering phenomena. In order to enhance these parameters, DSSC can be made by frequently ordered  $\text{TiO}_2$  nanotube arrays [8].

According to Gratzel and Brian O'Regan they determine a PC technology made from the materials which their purity gradients vary from low-medium values. Through low cost fabrication methods which exhibits a commercially energy-conversion efficiency. This cell made with  $\text{TiO}_2$  transparent film with the thickness of 10 nm. the area of the film surface and the spectral properties of the dye mainly effect the circumstance of solar energy flux (%46) and the light conversion efficiency is high (over %80). A range of the total energy conversion is 7.1-7.9% in simulated solar light and 12% in adsorbed daylight [9].

Zainun et al. reported about  $\text{Cu}_2\text{O}/\text{TiO}_2$  heterojunction solar cells made by using electrochemical deposition (ECD). They demonstrated simple and low cost of solar cells by used ECD methods. However, its efficiency is still lower (less than 0.1%) [10].

Li and Wang et al. using  $\text{TiO}_2$  nanoparticles less than 20 nm prepared dye sensitized solar cell. The efficiency of the cells depend upon the size and crystallinity of the particles [11].

Murakami, Gratzel and Ito found that optimization the thickness of the TiO<sub>2</sub> layer acting as the working electrode affect both photo voltage and photocurrent of the device coated on the TiO<sub>2</sub> photo anode by an antireflection film results in enhancement of the photocurrent. Each of these components of film fabrication exerts a significant influence on the overall photovoltaic parameters of the devices resulting in improvements in the net energy conversion performance [12].

During the formation of thin film the coating technique is very important part. One of the good feature of the thin film solar cell is various simple or sophisticated deposition techniques can be possible. According to working condition or application area the coating technique can be varied.

For manufacturing TFs various methods have been used to fabricate thin films. But generally thin film deposition techniques divided in two groups; chemical and physical coating methods. Chemical vapor deposition, sol-gel, spray pyrolysis, atomic layer epitaxy and spin coating which are application of chemical coating technology. Physical coating techniques are separated into two class; sputtering and evaporation such as ion beam sputtering, magnetron sputtering, vacuum evaporation, electron beam evaporation and laser evaporation [13].



## 1.3 Chemical Coating Techniques

### 1.3.1 Chemical Vapor Deposition(CVD)

In CVD technique vapor phase components react with each other. End of the this reaction a solid film occurred on the surface. This process is carried out with the presence of thermal and radiation energy the pressures vary from 0.01 to 1 bar and the temperature values are between 200°C to 2000°C.

During the CVD process in reaction chamber, there is an inert gas which mostly used Ar react with the gaseous precursor components. End of the process, the solid is formed with two ways. As a coating solid, the reaction proceeds heterogeneously but as a powder solid, the reaction proceeds homogeneously. (In chamber the formation of films occur with heterogenous and homogenous reaction. Coating is done with heterogenous but for the powder formation happened with homogenous reaction) [14].

Fundamental aspect of this method is chemical reaction; therefore, the basic parameters of coating process and the reactions of the components should be properly examined. There are numerous types of chemical reactions occurred during this process. They are oxidation, pyrolysis, reduction, hydrolysis, synthetic chemical transport reaction etc [14].

CVD processes are essential techniques that used numerous applications such as refractory and other metals coating. CVD is also used for coating of semiconductors, borides, nitrides, carbides and oxides. Another important property is at the end of the deposition step the difference between the density value of coated material and the material common theoretical density is quite small. And also the material can be obtained with high purity, high thickness and the surface also has good adhesion properties. In this technique the chemical abilities of the substrate are very important. Substrate material must be chemically inert at high temperatures and its structure has to be durable and must not be degradable with high temperature points [14].

### 1.3.2 Sol-Gel Deposition Techniques

Colloidal solid particles within the size of 0.1-1  $\mu\text{m}$  dispersed in a liquid. Suspension of the particles occurs with the Brownian motions. Then two of the phases; liquid and solid are dispersed in each other. End of this chemical events a sol state is occurred. Sol state presents a solid network containing liquid components. The sol-gel coating method follows four stages. For the first stage to form a sol, the solid particles dispersed in a liquid. Then for the coating step a deposition is performed with 3 different ways. These techniques are spray coating (SC), dip coating (DC), and spin coating. After that the colloidal sol particles are polymerized and with removal of the stabilizing compounds. Then producing a gel state which in a structure of a continuous network is completed. Organic or inorganic components remains and pyrolyze at the final heat treatments and form an amorphous or crystalline deposition.

There are some advantages of sol-gel technology.

- ✓ It is possible to produce thin band-coating to provide perfect adhesion between the substrate and the coating
- ✓ For provide corrosion resistance layer, thick coating can be produced.
- ✓ Materials are shape into complex geometries in a gel state.
- ✓ High purity products are obtained with this coating method. Also the sol and the gel composition can be controllable.
- ✓ For the sintering step, the temperature can be kept low for example 200-600°C
- ✓ Despite the process is a very simple, economic and effective, high quality coating can be obtained.

Besides them this technique has many disadvantages and some limitations due to the weak bonding, low wear-resistance, high permeability, and difficult controlling of porosity this technique used in only small scale production, not suitable for full industrial production. The maximum thickness of coating is 0.5  $\mu\text{m}$ . Above this value the trapped organics caused failure during thermal treatment. And also substrate

material is very important in this technique. Thermal expansion property of the substrate limits the application of sol gel coating [15-18].

Sol gel coating technique is divided into 5 classes.

### 1.3.2.1. Dip Coating Method:

Dip coating is one of the most desirable sol-gel coating technique that used by many researchers. In this process a substrate material is dipped in a liquid, hold in liquid with enough time than pulled with a specified speed. The experiment is carried out under atmospheric conditions and controlled temperature.

Dip coating process divided into basically three steps:

1. Dipping and holding time: the substrate is dipped into a transparent precursor solution at a constant speed than waited enough time for the interaction of the substrate with the coating solution is occurs. And so the sols reached every point of substrates.
2. Deposition and drainage: The substrate is pulled upward at a constant speed. By the way excess liquid drained from the surface and the film deposition is occurred.
3. Evaporation: evaporation of solvent from the fluid which can be promoted by heat drying. Than subsequent heat treatment burned out the residual organics and induced crystallization of the functional oxides [19].

The process of dip coating is schematically represented below.

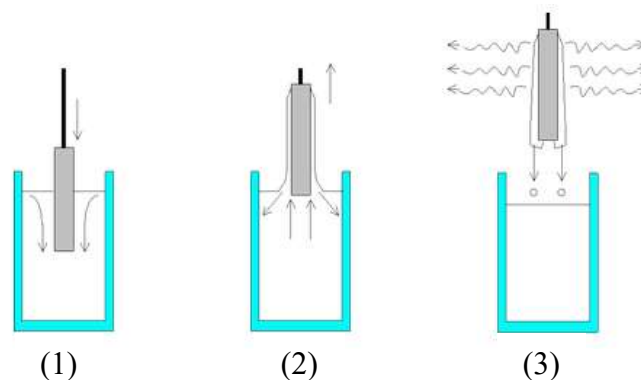


Figure 1.6 Coating steps of dip coating process (1) dipping (2) immersing (3) evaporation

In dip coating process, evaporation of the solvent and destabilization of the sols controlled by the atmosphere and then with the solvent evaporation, gelation process occurs. Finally because of the particles, which in the size of nanometer range in the sols, transparent film is formed. The gelation process during dip coating is represented in Figure 1.7.

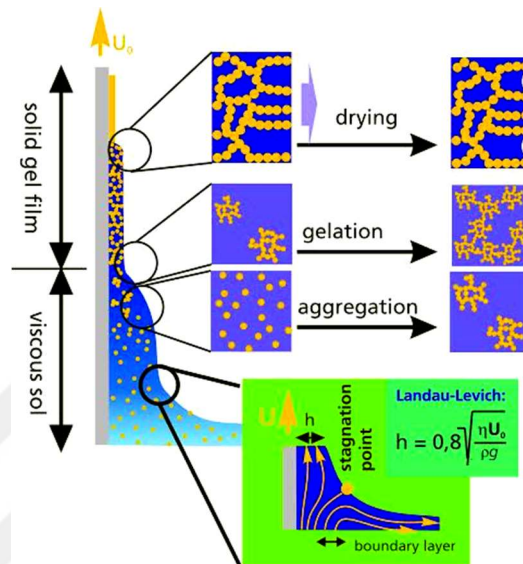


Figure 1.7 Schematic representation of dip coating process

The resulting film must be dense. And this densification obtained by thermal annealing. The annealing temperature determination is depends on the composition and this temperature is limited by the properties of the substrate.

The thickness of coatings is mainly depends on the substrate withdrawal speed, the viscosity of the liquid, and the solid content. The forces which are effective on the withdrawing step of the coating are represented below.

1. Viscous drag upward on the liquid by moving substrates
2. Gravity forces
3. Resultant force of surface tension in the concavely shaped meniscus
4. Inertial force of the boundary layer liquid arriving at deposition region
5. Surface tension gradient
6. The pressures of conjoining and disjoining process (important for films less than  $1\mu\text{m}$  thick).

The processes of dip coating are used for plate, glass and bulbs and have also been improved for curved surfaces like eye glass lenses. Besides all of them dip coating technique is applying a scratch resistant coatings for plastic substrates [20].

### 1.3.2.2. Spin Coating Method

Spin coating method is another technique of sol gel deposition. In this process the substrates rotated around an axis which must be vertical to the coating area. This is very simple and rapid process. Due to the centrifugal force spin coating provides very uniform coating on the surface of the substrate. There are four stages of spin coating process shown in figure given below. They are;

1. deposition of sol,
2. spin up,
3. spin off and
4. gelation by solvent evaporation.

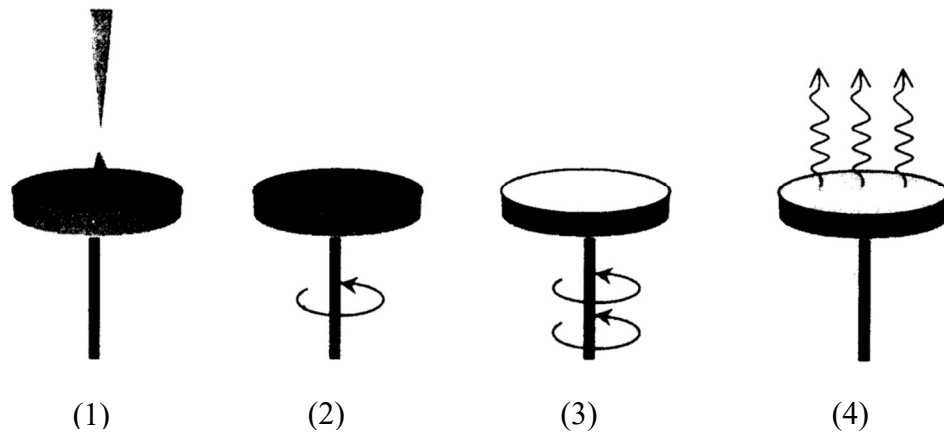


**Figure 1.8** Schematic diagram of the stages of the spin coating process [20]

In spin coating process owing to centrifugal force the coatings are tend to be more uniform and thinner than coating of dip coating process. The shape of the substrates does not matter in spin coating.

The rheological parameters of the coating limit mainly effect the quality of coating. Rheology is the parameter that relies on particle shape, temperature, solvent, concentration and particle interaction. Reynolds number of the surrounding atmosphere is another important parameter. High Reynolds number means high turbulence. If the rotation velocity is in a range that the atmospheric friction leads to high Reynolds numbers, disturbances in the optical quality are observed [20].

#### **1.3.2.3. Spray Coating Method**

Spray coating is known as an industrial method for organic lacquers. Coatings of irregularly shaped glass such as pressed glass parts, lamps or container glass are also possible with spray coating process. This technique is advantageous because it is fast and waste of sols is quite small.

In spray coating method very fine droplets which are in nanometer range are sprayed onto a substrate surface and due to these fine droplets very homogenous coatings can be obtained. Because of the high reactivity of these particles when hitting the hot surface, a continuous glass film can be formed [20].

#### **1.3.2.4. Flow Coating Processes:**

A Figure 1.9 is given below shows the flow coating process schematically. In flow coating process, the coating material is poured over the substrate to be coated. The thickness of coating is depends on the angel of slope of the substrate, viscosity of coating material and the evaporation rate of solvent. This method is used for automotive glazing application and functional coating application. For more homogenous coatings the spinning of the substrate process can be employed after the coating step [20].

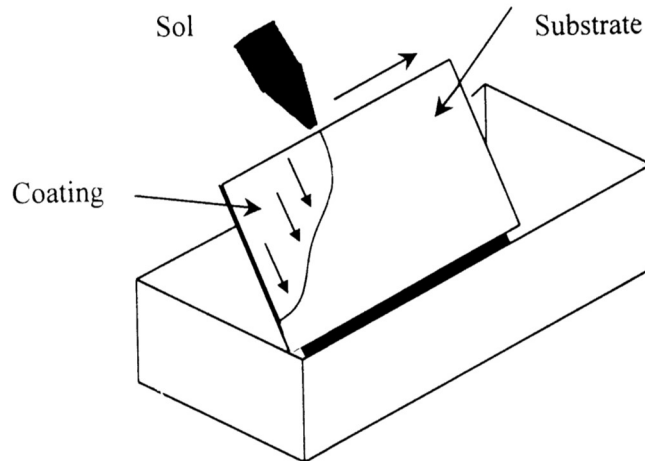


**Figure 1.9** Schematic diagram of the flow coating process [20]

### 1.3.2.5. Capillary Coating:

Spray and spin coating process are characterized by the fact the coating material cannot be brought all onto the substrate. So, in spray coating process more than 100% overspray is obtained, and similar amounts are wasted with spin coating. To overcome these wasted problems this method is developed. The capillary coating process provides solution reservoir collecting the excess of fluid and a pumping system to ensure a continuous solution feed during the deposition travel besides the coating. The coating thickness is depends on the deposition rate. Schematic representation of this process is given below [20].

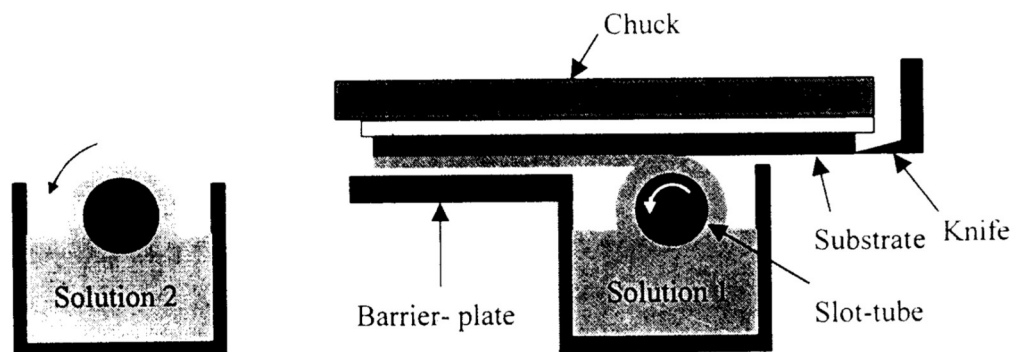


**Figure 1.10** Schematic representation of capillary coating [20]

### **1.3.3 Spray Pyrolysis Technique**

Spray pyrolysis is a sophisticated and useful technique. Spray pyrolysis technique is used in production of thin and thick films, application of ceramic coatings and wide variety of powders. Metal oxide, chalcogenide and even metal films have been produced by this technique. Spray pyrolysis is very simple and economic process which does not need high-quality substrates or chemicals. For dense, porous and multi layered films the method of spray pyrolysis can be feasible and very important method for solar cell application [21].

Typical spray pyrolysis equipment consists of an atomizer, precursor solution, substrate heater, and temperature controller. In spray pyrolysis process there are several types of atomizers used for coating such as air blast (the liquids exposed to a stream of air) ultrasonic (ultrasonic frequencies provides fine atomization) and electrostatic (the liquids exposed to a high electric field).

In spray pyrolysis, there are parameters that strongly affect the quality and the properties of the film. One of the most important parameter is the surface temperature of the substrates. When the substrate temperature increases, we could obtain the films which are rougher and more porous and also the temperature is too low the films might cracked. The deposition temperature also influences the crystallinity, texture, and other physical properties of the deposited films. Other major parameter is precursor solution which affects the morphology and the properties of the deposited films. In addition, the film morphology and properties can be strongly changed by using various additives in the precursor solution [21].

## **1.4 Physical Coating Techniques**

### **1.4.1 Sputter deposition**

Sputtering is the ejection of atoms by the bombardment of a solid or liquid target by energetic particles, mostly ions. Sputter deposition is a commonly used technique to deposit thin films on substrates. This technique is part of the class of physical vapor deposition techniques. The method is based on ion bombardment of a source material, the target. Ion bombardment results in a vapor due to a purely physical



process, i.e. the sputtering of the target material. The target can be powered in different ways, ranging from dc for conductive targets, to rf for non-conductive targets. This technique is applied in both research laboratories and industrial plants to deposit a lot of materials.

In this technique the interaction between the ion and the target, is a first priority. Sputtered target atoms are ejected with substantial kinetic energy, of the order of or larger than bond energies, and hence can significantly affect film growth kinetics and microstructure. Thus, energy loss mechanisms during transport in the gas phase are important [22].

In a characteristic sputtering system positive ions are move from plasma to a target that is at a negative potential with respect to the plasma. (Figure 1.6.)the ions hit the target surface due to an energy coming from the potential drop between the target and the plasma. The surface of target is considered as the source of material. The films are grown on target surface. And also the sputtered material is liberated from the bombarded surface that finally formed as a film. At the target surface many other events can be occurred. They are, secondary electron emission, secondary positive and ion emission, emission of radiation, heating, chemical dissociation or reaction and others. These events may influence the film growth.

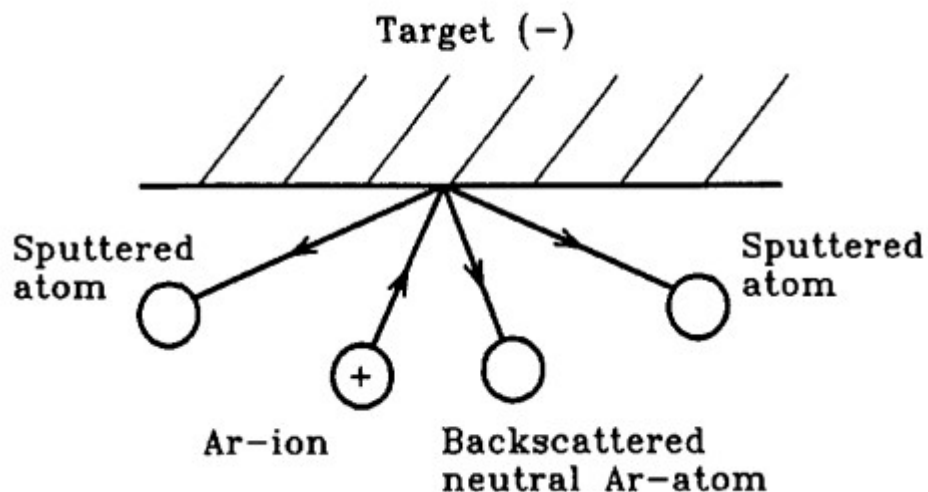


Figure 1.11 Sputtering mechanism [23]

In sputtering principle, clean substrate must be used prior to deposition process of film. The substrates are cleaned and their surfaces are free from the grass and the other surface contaminations before the substrates are put into vacuum chamber [23].

Types of sputtering techniques are; Ion beam sputtering, magnetron sputtering, reactive sputtering.

#### **1.4.2 Evaporation deposition**

Evaporation is the common and very old method of coating thin films. Among physical vapor deposition techniques thermal evaporation is the longest standing tradition. [24]

In evaporations technique, material source is heated to high temperature with thermal or electron beam methods and evaporated in a vacuum chamber. Through the high vacuum the vapor material transport to the substrate and stick onto the surface. Then the vapor material back to the solid phase thus the coating through the evaporation is completed [25].

A typical evaporation system is consists of an evaporation source (which can be a thermally heater, electron beam, laser beam, etc.) source material, the substrates material and the vacuum chamber. The substrate is placed at a suitable distance facing the source of evaporation. In a high vacuum chamber ( $P < 10^{-5}$  Torr) substrate material is heated with resistive or e-beam sources. And also high vacuum is performed for minimize the collisions of source atoms with background things (light). Desired material is in vapor phase, transports the target surface in vacuum atmosphere. Film thickness must be controlled with using a quartz balance because the deposition process can not be performed again. Physical surface interaction force are too fast ( $>1\mu\text{m}/\text{min}$ ). High sticking coefficient which means atoms stays wherever it hits, causes poor coverage due to the limited surface migration. Because of this situation with this method desired densely film could not be produced. But this also makes this process very advantageous choice for nanofabrication using liftoff process [25].

In evaporation techniques deposition rate is determined by emitted flux and by geometry of the source and wafer [25].

Evaporation techniques is offers us some advantages such as high film deposition rates, due to the involving high energy particles substrate materials damage is less, high purity of film, etc. This method has some disadvantages: control of film composition is quite difficult, the technique does not capable of in situ cleaning of substrate surfaces, step coverage is difficult, etc.

Evaporation techniques are divided into 3 groups. They are; Vacuum evaporation, Electron beam evaporation, laser evaporation [26].

In thin film studies, choosing deposition techniques and optimizing the better conditions is very important step. The studies with using different coating techniques are available in literature. Nanocrystalline TiO<sub>2</sub> thin film prepared by chemical vapor deposition techniques. CVD parameters optimized for better thickness and the conclusion is for better thickness homogeneity appropriate conditions are high Ar flux and longer plasma distance [27].

Transparent conductive Nb-doped TiO<sub>2</sub> films deposited by reactive sputtering method. For the oxidation of the substrate surface is controlled by the reactive sputtering feedback system across the entire range of O<sub>2</sub> flow ratio in the transition region, enabling a stable and highly reproducible deposition. the reactive sputtering with an impedance feedback system successfully controlled the metal-oxygen stoichiometry precisely [28].

Sn-doped ZnO thin films with 0%, 0.5%, 1%, 1.5% and 2% Sn were grown by spray pyrolysis method on glass substrates under optimized conditions. Low concentration Sn-doped ZnO thin films grown on glass substrates by the simple and low cost spray pyrolysis technique, the doping improves the optical properties of the films, especially for a 0.5%Sn concentration, facilitating the incorporation of such films into low cost optoelectronic devices [29].

Transparent conducting phosphorus fluorine Co-doped tin oxide (SnO<sub>2</sub>:(P,F)) thin films have been deposited onto preheated glass substrates using the spray pyrolysis

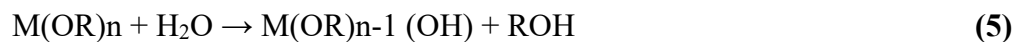
technique by the various dopant quantity of spray solution. The physical properties of the prepared films with various levels from very low to high doped was investigated. It was observed that the physical properties of the films strongly depend on the doping level. The study shows that for multi doping of semiconductor films, very low level doping is necessary [30].

As we can see above, tens of coating techniques are mentioned in literature. To fabricate TiO<sub>2</sub> films, there are number of methods including sputtering, chemical vapor deposition, and sol-gel process. The sol-gel technique offers many advantages over other deposition techniques due to the use of very simple and inexpensive equipment [31,32].

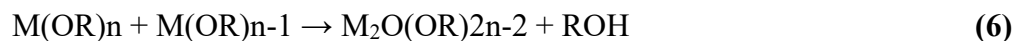
### 1.5 Synthesis Reaction of TiO<sub>2</sub> Nanoparticles by Sol-Gel Method

TiO<sub>2</sub> nanoparticles are synthesized with sol-gel method, using titanium based chemicals as a precursor. Successfully synthesized TiO<sub>2</sub> nanoparticles are reported. The sol-gel technique is most useful methods due to its possibility of obtaining metastable structure at low reaction temperatures and perfect chemical homogeneity. In sol-gel process TiO<sub>2</sub> is obtained by the reactions of hydrolysis and polycondensation of titanium alkoxide (TiOR)<sub>n</sub> to form oxopolymers, which are transformed into an oxide network. These reactions can be presented in below.

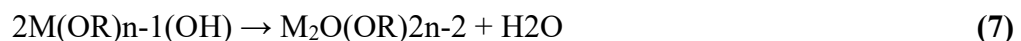
Hydrolysis;



Condensation Dehydration;



Dealcoholation;



The overall reaction is;



Ti is represented by M, alkyl group shown by R. the relative rates of hydrolysis and condensation strongly depended on the structure and properties of metal oxides.

Important factors that effect the formation of metal oxides are reactivity of metal alkoxides ,alkoxides ratio, pH of sols, nature of solvent, additives and reaction temperature. Due to the this parameters different surface chemistry and microstructure can be produced [33].

Several pH-dependent rate profiles have also been reported for the hydrolysis and condensation reactions, where it has been found that reaction rates are largely dependent on pH, For instance, at pH = 7, molecular hydrolysis occurs at a slow rate, while molecular condensation occurs at a fast rate. It is this inverse relationship between the rates of the hydrolysis and condensation reactions that must be taken into account in controlling the kinetics of the reaction and therefore controlling the ultimate network structure [34].

About pH effect, some studies are available in literature. ZnO films deposited at different pH values. A strong influence of pH on the crystalline growth is clearly observed. The surface morphology of the films is found to improve with increase in increasing pH values. The size distribution of grains appears to be less homogenous for lower pH values. The grain size increases with increase in pH of the precursor solution. This study shows also the increase in pH values of range 4,6,8 and 10 decreases the band gap energy from 3.32 to 3.14 eV [35].

Another study shows that the surface morphology of the films is greatly dependent on the type of the sol. the film from the base sol consists of agglomerated titania particles which may cause the surface to be non uniform. The films from the acid sols, however, are very dense with much smoother surface. The sol pH influences thickness and grain size. Indeed, grain size and thickness increase with increasing the sol pH. It should be mentioned that film weight for the acid and base sols are 0.2 and 0.5g respectively. The surface of the film deposited from the base sol is composed of agglomerated titania particles while distribution of the particles on the surface is non uniform. The roughness of the surface which is about 16 nm. However, the film from the acid sol is dense and its surface is smooth and uniform, in this case the roughness profile of the acid film is 6 nm [36].

According to other experiment, the thin films prepared at pH 3 showed homogeneous and well covered on the substrate. These films consist of small grains (0.2  $\mu\text{m}$ ) which lead to deposition of smoother films (17 nm). As the pH increases up to 7, the number of grains decreases and larger grain size could be obtained. The roughness values of 31 and 56 nm have been observed for samples prepared at pH 5 and 7. Root mean square (RMS) roughness is defined as the standard deviation of the surface height profile from the average height, is the most commonly reported measurement of surface roughness “(Jiang et al. 2005)”. The surface roughness of the film is unavoidable since grains were grown with different sizes and spherical in shapes. On the other hand, the fine grains were observed for the film prepared at pH 9. The grain size of the film was estimated to be 0.15  $\mu\text{m}$  in diameter, which is much smaller than the grain size of the film prepared at pH 3. Therefore, the pH leads to change of the film morphology. The thickness of the film with pH for ZnS thin films. It is clear that the thickness of the film increased as the pH was increased up to 7. However, the films deposited at pH 9 produced thinner films compared to other pH values [37].

# CHAPTER 2

## EXPERIMENTAL PROCEDURES

### 2.1 Materials

#### 2.1.1. Indium tin oxide (ITO)

ITO is a complex compound that includes indium, tin and oxygen elements in different proportions. The oxygen contents can varies and according to this contents ITO structure may be ceramic or alloy. The formulation of ITO is 74% In, 18% O<sub>2</sub>, and 8% Sn by weight. The compounds of oxygen saturated compositions are so usual, but unsaturated compositions are called oxygen deficient ITO. In thin layer form, it is colorless and transparent but the structure in bulk form it is yellow to grey. It behaves as a metal like mirror in spectrum infrared region [37].

ITO is most used TCO compounds. The main reasons of this usage are, its electrical conductivity and optical transparency. Due to low electrical resistivity properties (10-4  $\Omega$ ) ITO thin films are worked as n-type semiconductors. The reason of low resistivity value of ITO thin films is high carrier concentration. Additionally, ITO is a wide band gap semiconductor ( $E_g=3.5-4.3$  eV) so that in the visible range of the electromagnetic spectrum, it shows high transmittance (>80%). The optical and electrical properties of ITO are mainly depends on the concentration of Sn<sup>+</sup>.

The areas in which ITO used extensively are;

- Flat panel displays (FPD)
- Antireflection coatings
- Heat reflecting mirrors
- Gas sensors
- Energy efficient windows
- Solar cells

There are various techniques to produced ITO thin films; [38].

- dc and rf sputtering
- Spray pyrolysis
- Ion-assisted deposition
- Electron beam evaporation
- Pulsed laser deposition
- Sol-gel process

In a powder form, indium tin oxide (ITO) is yellow-green in color, but it is transparent and colorless when deposited as a thin film at thicknesses of 1000-3000 angstroms. When deposited as a thin film on glass or clear plastic it functions as a transparent electrical conductor [39].

ITO glass slides were used as a substrate for fabricating polymer solar cells based on blends of polymeric semiconductors and organic light emitting diodes (OLEDS). Transparent heater arrays were fabricated by etching on ITO substrates for a cantilever-free printing tool [40].

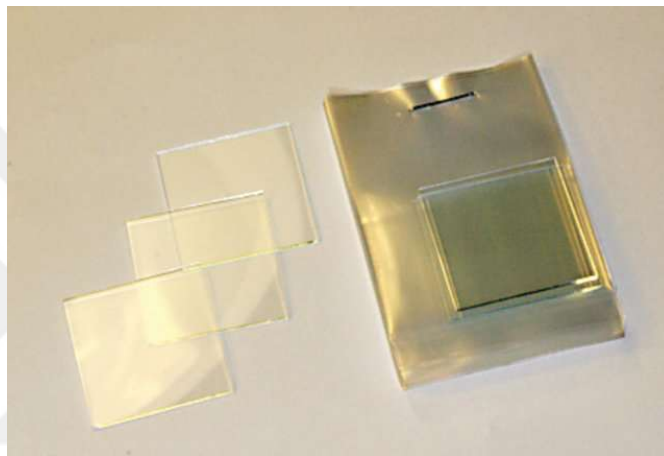


**Figure 2.1** Indium Tin Oxide Glass

Properties of ITO coated glass is given table 2.1 below.

**Table 2.1** Properties of ITO coated glass(Sigma Aldrich)

<b>description</b>	slide
<b>surface resistivity</b>	8-12 $\Omega$ /sq
<b>L <math>\times</math> W <math>\times</math> thickness</b>	25 mm $\times$ 25 mm $\times$ 1.1 mm
<b>transmittance</b>	84% (nominal at 550nm)
<b>refractive index</b>	$n_{20/D}$ 1.517

Chemicals which containing  $\text{TiO}_2$  are obtained from Alfa-Aesar. They are ordered for solution preparing of sol gel coating step. The list of chemicals that we ordered for solution preparation is shown in Table 2.2.



**Table 2.2**List of chemicals

Name	Company	Linear Formula	Molecular Weight
Titanium ethoxide	ALDRICH	Ti(OC <sub>2</sub> H <sub>5</sub> ) <sub>4</sub>	228.11
Titanium butoxide	Alfa-Aesar	C <sub>16</sub> H <sub>36</sub> O <sub>4</sub> Ti	340.36
Titanium methoxide	ALDRICH	Ti(OCH <sub>3</sub> ) <sub>4</sub>	172.00
Titanium nitride	Alfa-Aesar	TiN	61.91
Methanol	ALDRICH	CH <sub>3</sub> OH	32.04
Acetyl acetone	ALDRICH	CH <sub>3</sub> COCH <sub>2</sub> COCH <sub>3</sub>	100.12
Hydrochloric acid	ALDRICH	HCl	36.46
Acetic acid	ALDRICH	CH <sub>3</sub> CO <sub>2</sub> H	60.05
Potassium Hydroxide	ALDRICH	KOH	56.11

## 2.1.2. Sample preparation

### 2.1.2.1 Solution

Solutions prepared with TiO<sub>2</sub> containing chemicals, acetyl acetone (chelating agent) and methanol (solvent).

According to solubility properties of the mixing components amount of acetyl acetone can be increased with little amount.

Solution is mixed with the magnetic stirrer between 2 and 24 hours, according to solubility properties of the components.

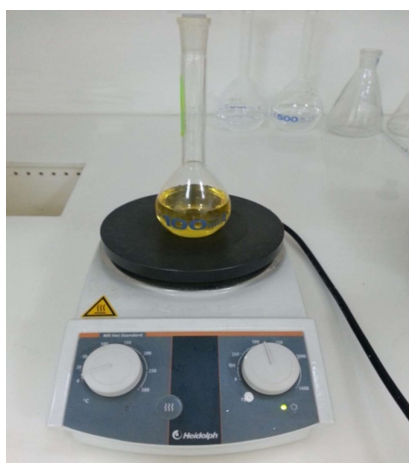


**Figure 2.2**The resulting solution is totally homogenous.

As a  $\text{TiO}_2$  based chemicals we used titanium ethoxide, titanium bütioxide, titanium metoxide and titanium nitride. Titanium methoxide and bütioxide are very suitable components for coating solution due to their good solubility properties.

On the other hand, because of the chemical situation of the titanium ethoxide, it was not possible to solve it, and also solution is prepared with titanium nitrate we cannot achieved complete dissolution.

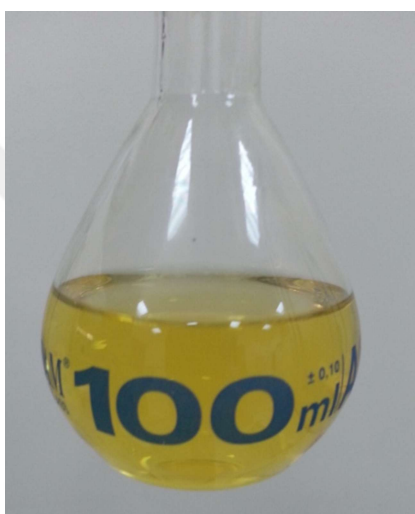


**Figure 2.3** The solution prepared with Titanium methoxide is fully transparent.

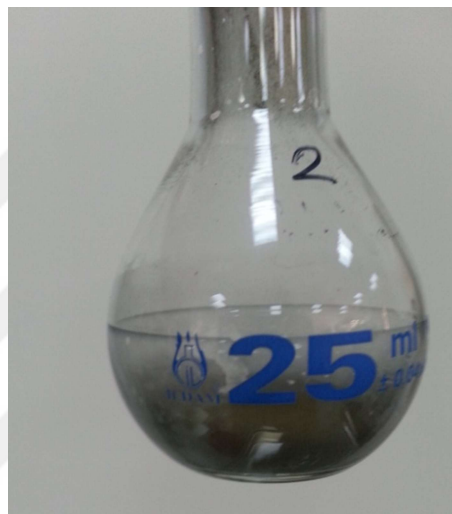


**Figure 2.4** The solution prepared with titanium nitrate cannot be solved completely

### 2.1.2.2 Ph Value of Coating Solution

We are especially focused on the ph effect on the surface properties of thin film. For this reason solutions with different pH values prepared step by step. The pH value of the solution is measured by pH meter which is trade mark of pL-700PD bench pH meter.



**Figure 2.5** Desktop type Ph meter

The desired pH value is achieved by adding acetic Acid. Because of the pH ranges arranged in a quite small value, acetic acid is added with a millimetric burette. By using a strong acid, solution preparation process would be very difficult. That is why we used acetic acid.

Solution pH values vary between 3,5 - 5,0. For dense and non porous film coating, the solution pH values must be in acidic limits [19]. After the acid addition process the solution is mixed for 24 hours.



**Figure 2.6**Solutions with different pH values

After the solution preparation the coating step is performed. The coating technique is sol gel dip coating method.

### **2.1.2.3 Drying/Firing the Coating**

The furnace is made for only coating process. In a vertical position furnace has a chamber with equal temperature distribution. For the coating step the furnace temperature is setted at 450 °C this temperature kept constant during the coating process.



**Figure 2.7.** Vertical Drying Furnaces

#### **2.1.2.4 Samples**

ITO glasses with 25\*25 mm size are cleaned firstly, than without doing any operation samples pulling into the vertical furnace chamber than hold for 15 second for the purpose of removal the oxide residues on surface. ITO coated-glass substrates are ready for coating by thermal cleaning.

#### **2.1.2.5 Etching**

Coated films are used in solar cell so that efficiency measurement is very important at this point. For this reason the ITO substrates are etched with HCl+Zn mixture. In this way, indium tin oxide layer on the glass is removal and conductivity should be measured directly on the glass with multimeter.

### 2.1.2.6 Process

The solution which became totally homogeny, taken on the magnetic stirrer.

ITO coated glass dipped into the solution. The solution reaches every point of substrates. Then pull into the furnace. Coated substrates pull into the furnace heated before for the first gelation and formation of film. The coated glass holds for 15 seconds into the furnace. Thus, the first gelation process is carried out.

Amount/number of dipping can be varying according to after coating processing desired properties or characterization methods that will be applied. Forming of thin film can be seen in figure given below.

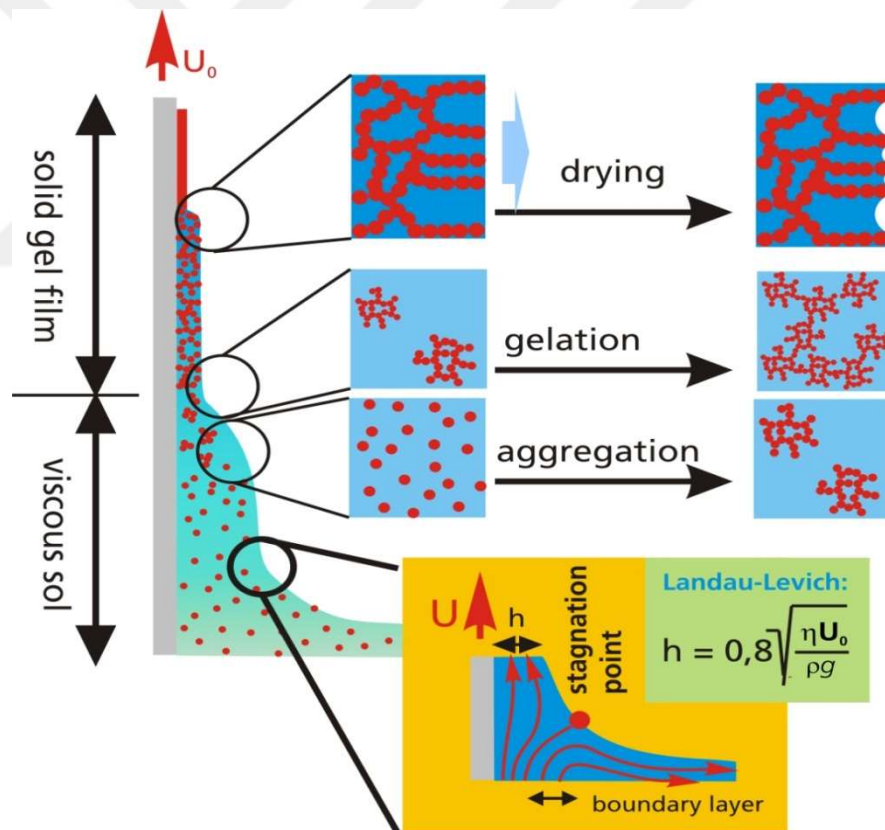


Figure 2.8 Sol-Gel Dip Coating Method

### 2.1.2.7 Annealing Process

After the coating and first gelation step the samples are put horizontal tube furnace for the final annealing process. During the step of determining the temperature range of annealing process, it must be considered that the samples are glass. Above the 600°C the glass samples may be cracked. For this reason, annealing temperatures are kept below this temperature point. For determine the effect of temperature and holding time on surface properties annealing process steps given table 2.3 below

**Table 2.3**Process steps

Process		
Temperature(°C)	Time(min)	pH
450	60	3.5
450	60	4.0
450	60	4.5
450	60	5.0



**Figure 2.9** Annealing furnace

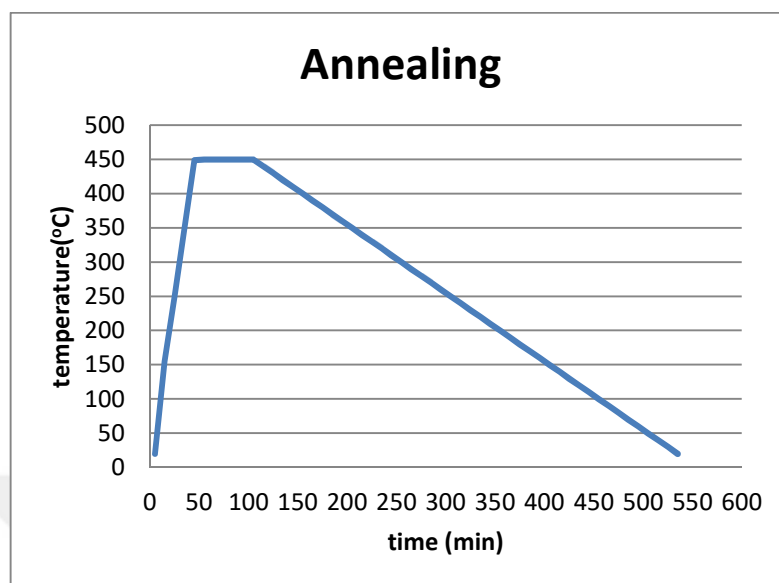


**Figure 2.10** Temperature profile applied for thermal treatment of the samples

After annealing process the samples are stored clean and pure conditions.

**Table 2.4** Sample list

Sample code	Annealing Temperature(°C)	Annealing time(Min)	pH	Precursor
<b>A1</b>	450	60	3.5	Titanium metoxide
<b>A2</b>	450	60	4.0	Titanium metoxide
<b>A3</b>	450	60	4.5	Titanium metoxide
<b>A4</b>	450	60	5.0	Titanium metoxide
<b>B1</b>	450	60	4.5	Titanium butoxide

## 2.2 Characterizations

### 2.2.1 Surface Analysis

If a scientist is studying samples at nano scale, obviously make sense the using atomic force microscopy (AFM), because of its properties such as most versatile and powerful microscopy technology. It is the surface characterization techniques and used for measuring the surface topography. This device can investigate the surface morphology from angstrom level up to 100-150 microns [41]. To observe the



surface properties of the specimen such as roughness at a high resolution, and to discriminate a specimen based on its mechanical properties (such as roughness and hardness) and, additionally, to carry out the microfabrication properties of a specimen (such as, an atomic manipulation), an atomic force microscope (AFM) can be used [42].

This technique is based on the interactions between the tip and the surface atoms. Working principle of typical AFM is rather simple. As can be seen in the Figure 2.10 A tip which is in the size of few microns level is placed end of the cantilever. These tip scanned over the sample surface. During the scanning process the interatomic forces ( $10^{-11}$ - $10^{-6}$  N) which are occurs between the surface and the tip, lead to deflection of the cantilever. This deflection measured with a probe to get the topography of the scanned area. With this way, the information about the growth mode, surface roughness parameters, types of surface defects and the volume/density of the surface defects can be measured from the AFM results [41].

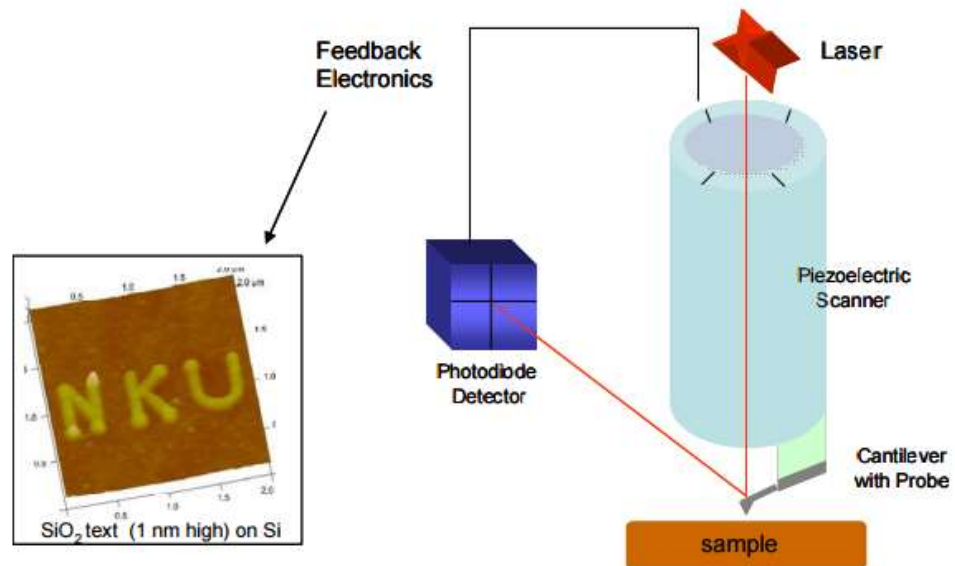


**Figure 2.11** Working principle of AFM instrument

The working principle of AFM is depends on 3 basic steps.

Surface sensing, detection method and imaging.

### 2.2.1.1 Surface Sensing

An AFM can scan the surface with three modes. They are contact mode, non-contact mode and tapping mode. The modes of analysis are determined by the distance of the sample surface to tip. A Figure 2.11. given below shows the interaction forces between the sample surfaces to tip versus the surface-tip distance.

For the first situation when the tip come near to the sample surface, the tip is attracted weakly by the surface. (right side of the curve) When the Surface-tip distance decreased, this attractive force increased until the atoms which are on the sample and the tip surface begin to repulse each other. As a result of the distance decreased slightly repulsive force increased and total force at a specific distance is equal to zero. (0) at this point the physical contact occurs between the tip and the sample. After this point attractive force dominates the repulsive force (left side of the curve). In contact mode the distance between the sample-tip is in a level of a few angstroms. So the tip is physically contacted with the sample surface and subjected to repulsive forces. ( $10^{-9}$  N) In this mode, surface topography is obtained by the deflection of the tip or the change difference of the surface height.

In non-contact mode the distance between surface-tip is approximately 50-150 Å. At this point attractive force is weaker than the forces at the contact mode and less sensitive the changes of surface height. The tip does not contact the sample surface but cantilever vibrates with specific frequency. When the tip approaches the surface the the changes of the frequency is measured. Using a feedback loop to monitor changes in the frequency amplitude due to the attractive forces than the surface topography can be measured.

In tapping mode, the cantilever is oscillated at its resonant frequency. The probe gently taps on the surface of the specimen. By maintaining constant oscillation amplitude o constant tip-sample interaction is maintained and an image of the surface is obtained. [42]

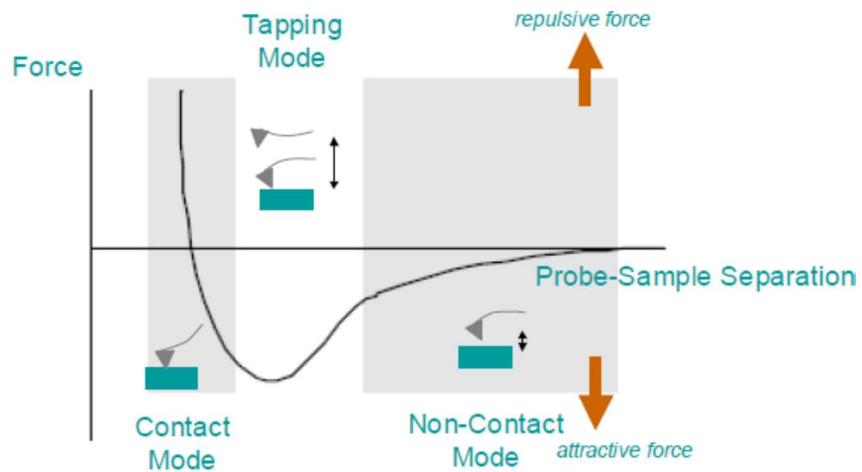


Figure 2.12 Schematic representation of interaction forces versus tip distance

### 2.2.1.2 Detection Method

For detecting the deflections of cantilever that caused from the surface features of the specimen, a laser beam is used. An incident beam reflects the surface and due to the slight changes which are encountered during the scanning of the specimen surface, are deflected the on the way of the reflected beam. For track this changes, a positive-sensitive photo diode (PSPD) is used. So, an AFM tips passed over a raised surface feature the resulting cantilever deflection and the PSPD recorded the subsequent change in direction of the reflected beam [43].

### 2.2.1.3 Imaging

An AFM images helps to achieve the topographical properties of a surface of specimen by scanning the cantilever over a region that we interested in. The deflection of the cantilever affected by the raised and the lowered features on the surface of the specimen, and it is possible to observe these features with help of PSPD. Using the feedback loop helps to control the height of the tip above the specimen surface thus, the atomic force microscope (AFM) able to produce a topographic map of the surface properties.

In our experiment we worked AFM with contact mode. The measurement parameters are given table below.

**Table 2.5**The analysis parameters of AFM

Head mode	NC-AFM
Source	Topography
Data Width	1024 (pxl)
Data Height	256 (pxl)
X Scan Size	5 ( $\mu\text{m}$ )
Y Scan Size	5 ( $\mu\text{m}$ )
Scan Rate	1.25 (Hz)
Set Point	-0.2
Data Gain	-26.433E-6 ( $\mu\text{m}/\text{step}$ )

### 2.2.2 Thickness Measurements

With improvements of thin film application in our everyday lives, a numerous of thin film thickness measurements have attracted a lot of attention from both researchers and manufacturers. Film thickness is very important parameter for material properties of thin films. For semiconductors, microelectronics, photonics, microsystems and the other engineering industries thickness measurements are excessive attention for researchers [44-45].

Many other various techniques can be used for measuring the thickness of thin films. Stylus profilometry, interferometry, ellipsometry, spectrophotometry and EPMA (Electron Probe Microanalyzer) are the few techniques, but not limited to, measuring thin film techniques. Also the proper measuring techniques to be used depending on the film characteristics are under continuous investigation.

Throughout the production of thin film process even during the deposition step, it is essential to have much information about the current film thickness and so the primary duty of the thin film technology is specification on thickness of the thin film and the rate of deposition [46].

A number of tools are used to measure properties such as surface roughness, texture and thin film thickness. Popular techniques to measure the thickness of thin films are such as stylus profilometry, interferometry, ellipsometry, spectrophotometry (XRF), Atomic force microscopy (AFM) and scanning electron microscopy (SEM), Electron Probe Micro Analyzer(EPMA). And the suitable method is chosen according to the film characteristic under ongoing investigations [47].

The stylus profilometer is the most common method to measure the thin film thickness. It is able to scan areas of tens of millimeters with a perpendicular range starting from few nanometers up to hundreds of microns. During the analyzing this tool contacts through the sample surface and able to cause a destruction of the surface of sample. This situation is the main disadvantage of stylus profilometer[48].

Atomic Force Microscopy technique is used measuring in nano scale and for a surface scanning. It is possible to scratch the surface of film with using the contact mode of AFM. Instead of contact mode semi-contact AFM measurement can be performed. Besides them,for measuring of thin film, the AFM technique is expensive and time consuming. Moreover, both contact and semi-contact modes of AFM are scanning within less than hundreds of microns area with approximately tens of microns displacement in the vertical direction. The advantage of this technique is not required the electronically conductive sample [48].

For thickness measurements ellipsometer is another tool that evaluates the film surface. Ellipsometry uses the fact that light undergoes some change in polarization when the reflection from a surface of a material. The polarization change is characteristic of the surface structure of the sample. Besides the ellipsometer is non destructive methods also in stu study which means there is no affection on the process from this tool. And also this method requires only a low-power light source. The parameters that ellipsometer can be determined that given below.

- Film thickness
- Anisotropy Retardation
- Refractive Index (n)
- Phase Difference
- Extinction Coefficient (k)
- Surface Roughness

Many thickness measurement methods can not be used the films which have small dimensions and intricate geometries. Under this circumstance for the thickness measurements the techniques based on scanning electron microscopy (SEM), scanning transmission electron microscopy or electron energy loss spectroscopy can be preferable [49].

These methods are destructive and the samples should be prepared with cross-sectional shape. Sample preparation for TEM and SEM by focused ion beam (FIB), the selection of sampling location is critical. Then the cross-sectional scanning images saved by the SEM built in FIB system [50-51].

An electron beam hit a sample surface, and the surface produced the secondary electrons as signal electrons. The signal intensity of electrons is dependent on the thickness of the measurement sample film thicknesses. The film thickness is reached 200 nm, the intensity of backscattered electron changes. Below 200 nm intensity rapidly decreases. The maximum depth of the electrons scattered from the sample is approximately 200 nm. If the sample is thicker than this depth, the signal is constant. If the film is thinner than this depth the signal volume is reduces.

Monitoring the back scattered electron intensity produces stable thickness measurements because the signal volume of backscattered electrons is less influenced by surface conditions than that of secondary electrons [52].

Thickness measurement is performed with SEM-FIB technique before with the same condition.

### **2.2.3 Chemical Measurements**

#### **2.2.3.1 XPS Analysis**

This method is one of the most admired surface characterization technique that also known as Electron Spectroscopy for Chemical Analysis (ESCA). XPS characterization technique has been in use extensively since it firstly developed by Kai Siegbahn. Because of the simplicity and ability in examination in chemical analysis with a high precisions and sensitivity this technique is used intensively.

As shown in Figure 2.12 XPS analysis, which uses X-rays as a photon source, is based on the photoelectric effect. So, as a probe source, X-ray source is used and electron analyzer analyzed kinetic energy of discharge electrons for obtained chemically resolved output. The electron energy analyzer consists of a sequence of electrostatic lenses, kinetic energy separator and a detector [53].

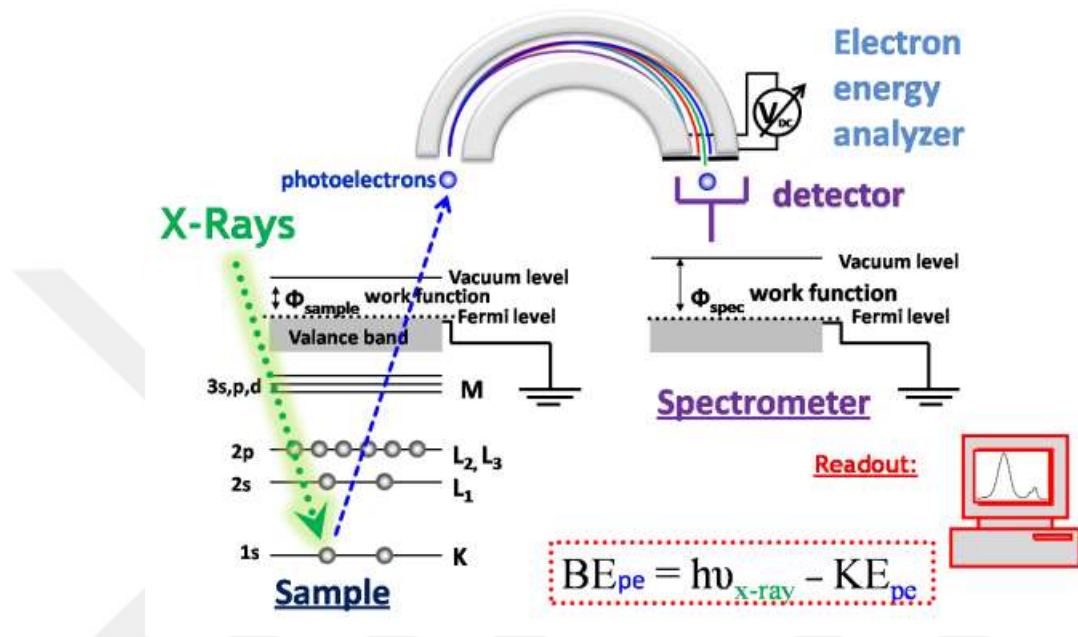


Figure 2.13 Working principle of XPS.

The XPS analysis must be done in ultra high vacuum (UHV) atmosphere to increase the possibility of photoelectrons reaching the detector is increased against getting lost. The photoelectrons are separated by the electronic lenses and the analyzer, according to their kinetic energies to reach the detector. The energetically separated photoelectrons, which pass through the electron energy analyzer for a certain time period, are counted by the detector. The previous step the binding energy value evaluated from the kinetic energy information. The binding energy is calculated from the equation of Einstein's relation

$$BE = h\nu = KE - \Phi_{\text{spec}} \quad (9)$$

The binding energy shown by BE, KE is the kinetic energy of photoelectron, and  $h\nu$  refers to the energy of X-ray photons.  $\Phi_{\text{spec}}$  is the work-function of the electron energy analyzer of the instrument and this parameter should be eliminated the equation for conductive samples [53].

XPS signals which are obtained from the binding energy of the photoelectron are varies, so XPS signals are classified and represent different atoms and provides distinct chemical and physical information about the sample [54].

The XPS device can analyze only a few atomic layers that are on the top of the sample surface. Due to the inelastic collisions of photoelectrons XPS is able to scans 1-20  $\mu\text{m}$  depth into the sample [54].

The areas of XPS can be in used for; Elemental analysis, Chemical state analysis, Quantification, Depth profiling [54].

- ✓ **Elemental analysis:** XPS technique is mainly used to evaluate the sample surface. Besides this, clear elemental determination of atoms is performed owing to the specific value of peak position. (Binding energy) Many elements characterized by with this way except for helium and hydrogen elements. The amount of binding energy also supplies information about orbital of the atom from which photoelectron is released. The peak area is also important. In XPS technique theratios of the relative area between two spin-orbit peaksfor each p, d, and f orbital have evident values as 1:2, 2:3 and 3:4 respectively.
- ✓ **Chemical state analysis:** XPS technique is able to determine the chemical state of the surface atoms of sample. Different chemical states are belongs to same elements in a sample might results shifting in the energies of binding. Different states of oxidation might cause some changes in the energy levels of core electrons in atoms than the kinetic energies of electrons can be effected. This shift is called 'chemical shift'.
- ✓ **Quantification:** The quantitative information about the sample surface is obtained out of the elemental analysis characterization by XPS. This determination of the sample surface in a range of 1 to 20 nm is done by calculating the relative atomic ratios by using the peak areas.



✓ **Dept profiling:** Depth profiling is the analysis of compositional on the vertical path through the surface plane of the specimen. 2 types of depth profiling methods are available; Destructive, Non destructive [54].



**Figure 2.14** X-ray Photoelectron Spectroscopy (UNAM)

XPS is the most sensitive chemical analyze device. It also provides etching with Argon before scanning. This etching carried out for cleaning the surface from residues, contamination and performed better phase analysis [53,54].

XPS analysis performed at Bilkent University which is trade mark of XPS Thermo K-Alpha. The scanning parameters are given below.

**Table 2. 6** Scanning parameters of XPS analysis

Parameter	
Total acquisition time	2 mins 16.1 secs
Number of Scans	2
Source Gun Type	Al K Alpha
Spot Size	400 $\mu\text{m}$
Lens Mode	Standard
Analyser Mode	CAE : Pass Energy 200.0 eV
Number of Energy Step	1361

### 2.2.3.2 XRD Analysis

X-ray diffraction is very important characterization method used in solid state chemistry and materials science. This technique provides very definitive structural information and so most preferable technique used for illumination of crystal structure. [55]

For determine the orientation of a single crystal or grain and find the crystal structure of an unknown material XRD scanning is performed. The size and the shape of the crystal structure and the distance between the crystal planes are also characterized with this method. The atomic planes of a crystal cause an incident beam of X-rays to interfere with one another as they leave the crystal. The phenomenon is called X-ray diffraction.

Many substances have a periodic structure and interatomic distance in crystal structure is in the range of X-ray wavelength. These reasons allow the XRD technique for illumination of the crystal structure. [56]

X-ray diffractometers are made up of three key instruments: a X-ray tube, a sample holder, and a X-ray detector. X-ray beams are generated in a way of producing electrons by heating a filament in the cathode ray tube. The electrons are accelerated on the way to a target by applied voltage, and the target material is being bombarded with these electrons. Lastly, when the electrons that were produced, have an adequate energy to excite inner shell electrons of the target material, characteristic X-ray spectra are generated. [57].

The electrons in an atom is scattered the light. The atoms which are placed in a crystal with a periodic array can diffract the light. The crystal structure shows the atomic arrangement of a material. The wavelengths of X ray are similar to the distance between atoms. The scattered X rays produces a diffraction pattern provides very clear information about the atomic arrangement within the crystal. Different arrangement of atoms caused different diffraction patterns [56].

Bragg Law is the easiest way to understand the essential conditions for production of diffraction. Diffraction only occurs in the angle values of which provide this equation [56].

$$n\lambda = 2d\sin\theta \quad (10)$$

As can be shown in figure,  $d$  is the space between the crystal planes,  $\theta$  is the incident angle,  $n$  is any integer and  $\lambda$  is the wavelength of the X ray beam. If  $n=0$  there is no diffraction can be observed. The value of  $n$  must be minimum 1 [56].

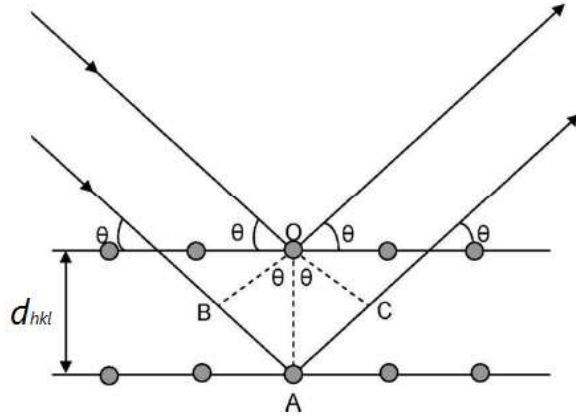


Figure 2.15 Schematic representation of Bragg Law



**Figure 2.16** X-Ray Diffractometer

XRD analysis performed at Bilkent University which is trade mark of XRD PANalytical Xpert Pro MPD. The scanning parameters are given below.

Parameters	
$2\theta$	0-90°
Intensity	0-120

# CHAPTER 3

## RESULTS AND DISCUSSIONS

### 3.1 Chemical Analysis

#### 3.1.1 XPS Characterization

XPS scanning is performed to evaluate the surface of the samples, chemical properties and analysis. Samples are prepared and put into the vacuum chamber. 30 minutes later experimental is finished.

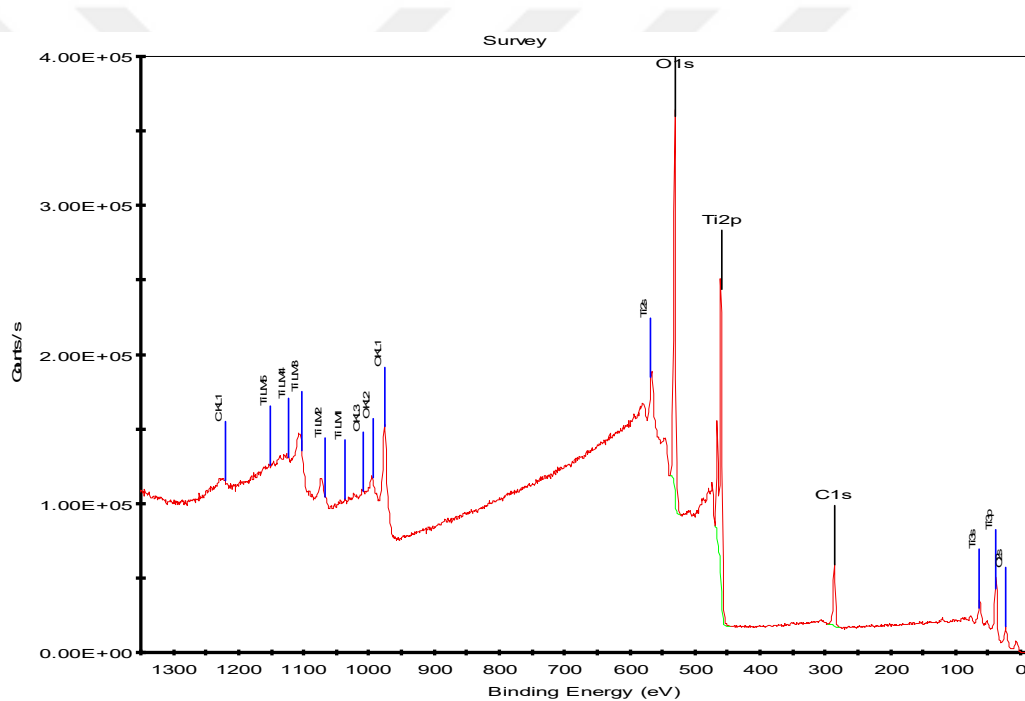
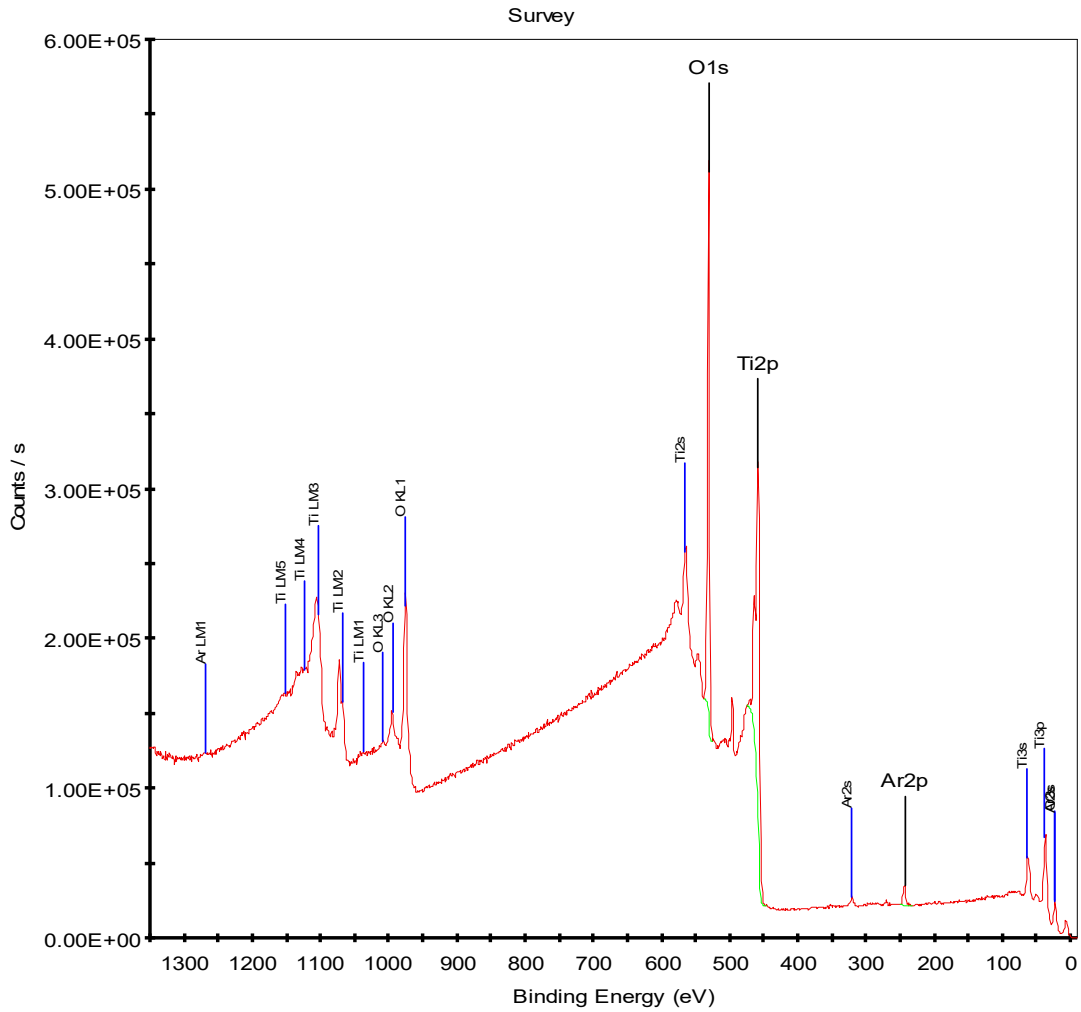


Figure 3.1 XPS scanning result of TiO<sub>2</sub> thin films

The first scanning data shows the peaks are about C are very sharp. (Figure) Top layers of the coating are containing high percentage of carbon. It is obvious that the surface of B1 sample is not clean enough. These contaminations may cause from the storage conditions of samples or the dirt coming from the operating environment.



**Figure 3.2** XPS scanning result of TiO<sub>2</sub> thin films after Ar etching

For the better phase analysis the peaks arising from in the presence of C should be reduced as much as possible. So, the surface was etched by Argon. According the scanning data, the Ti-TiO<sub>2</sub> bonds were observed significantly. The operation temperature of coating step is kept constant at 450°C. As it is shown in the figure 4 TiO<sub>2</sub> were formed noticeably but the crystallization process and transformation of anatase- rutil has not been occurred. The crystallization from amorphous to anatase and from anatase to rutil usually occurs in the temperature ranges of 450–550 °C and 600–700 °C, respectively [11]. The reason for that the phase transformation does not occur at the operating temperature which is lower than the phase formation temperature. Due to the heating limitation of glass substrate crystallization temperature must be kept under 550°C. Above that temperature glass substrate will be cracked.

As can be seen in the figure, the XPS scanning of the TiO<sub>2</sub> thin film, there are only the peaks of titanium and oxygen. Therefore, the structure of the film contains only titanium and oxygen atoms.

To determine the stoichiometry of the film, the data's, obtained from the XPS results, examined and the areas divided into appropriate Atomic Sensitivity Factor values than the ratio of the O<sub>2</sub> to Ti is obtained.

$$Ti = \frac{1618887.29}{1.8} = 899391.83 \quad (11)$$

$$O = \frac{1247272.85}{0.66} = 1889807.35 \quad (12)$$

$$\frac{O}{Ti} = \frac{1889807.35}{899381.83} = 2.101 \quad (13)$$

The result, 2.101 is, showed us TiO<sub>2</sub> is formed successfully [58].

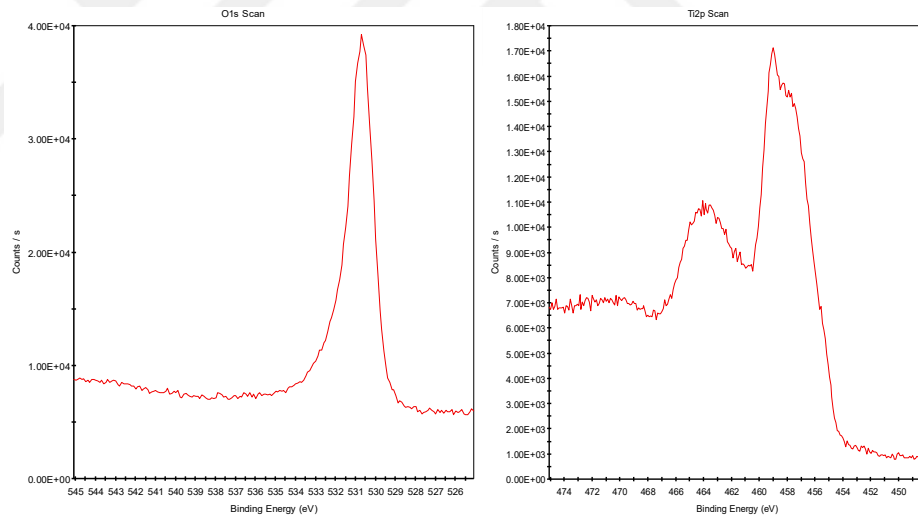


**Figure 3.3** Binding energy peaks of TiO<sub>2</sub> and O<sub>2</sub>

Figures given above shows that the binding energies of peaks which belong to Ti<sub>2</sub>p<sub>3/2</sub> and Ti<sub>2</sub>p<sub>1/2</sub>, are 459 eV and 464 eV also the binding energy of O<sub>1s</sub> that is detected in 530.95 eV. These findings are consistent with other studies in literature.

### 3.1.2 XRD Characterization

For XRD scanning, the substrate material must be conductive. But our samples are glass and as it is known ceramic materials are good insulator. So for the characterization of XRD, Al plate was used as substrate material, since it is not possible to get a XRD peak from thin film on glass substrate. TiO<sub>2</sub> thin film is coated on Al plate to get the same conditions. Before the characterization Al samples are first grinded and polished than coated with titanium butoxide.

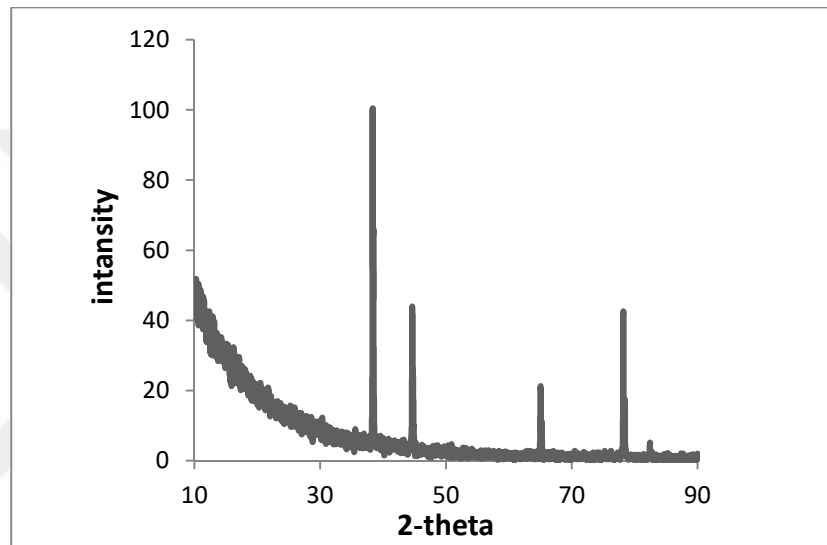


**Figure 3.4**XRD analysis results of thin films

According to first scanning results a position of the peaks are shows that there was too much background noise (figure given above). The peak density is too low. We cannot achieve to get reliable results. The data's must be recollected with more scans. For less noise and better phase analyses the experimental is repeated with scanning time was increased.



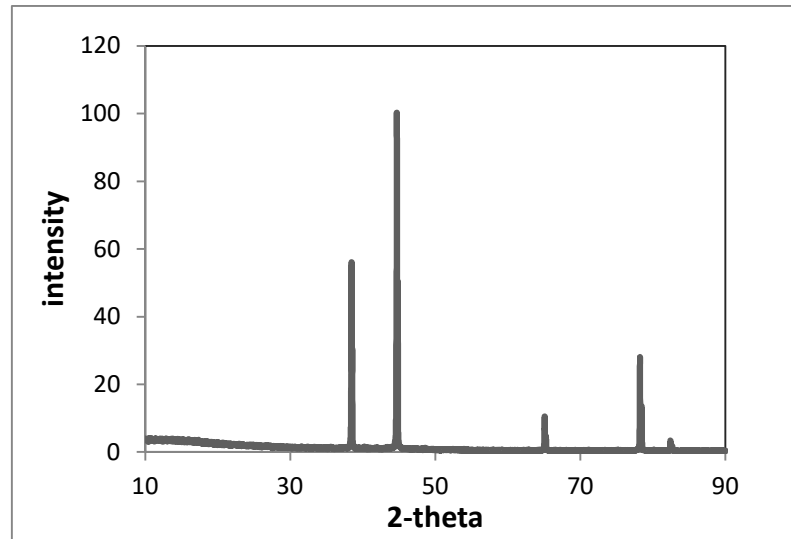


**Figure 3.4**XRD results of thin films second scanning result

Figure shows X-ray diffraction pattern of TiO<sub>2</sub> thin films prepared at Titanium butoxide with pH values of 4.5. As a substrate material we use Al plate. A crystallinity property of Al is very high, so the peaks shown in the diagram are almost arrived from the Al. since the operating temperature 450°C the phase transformation of TiO<sub>2</sub> does not occur. And also the low temperature cannot stimulate the crystallization process. A characteristic anatase peak which must be at about the point of 25° cannot be observed. This situation may be caused by high scanning speed or low operating temperature.

According to XRD results the peaks corresponding to the 38°, 45°, 65° and 83° 2θ all belong to Al substrate. The peak observed 78° belongs to TiO<sub>2</sub>. Thus, TiO<sub>2</sub> formation is observed successfully. But both XPS and XRD results, the phase transformation of TiO<sub>2</sub> cannot be observed.

## **3.2 Thickness Measurements**

### **3.2.1 SEM and Focused Ion Beam Microscopy Examinations**

Thickness measurement is done by FIB-SEM examinations. In another word thickness of the film which is coated with same conditions of this work is measured [59].

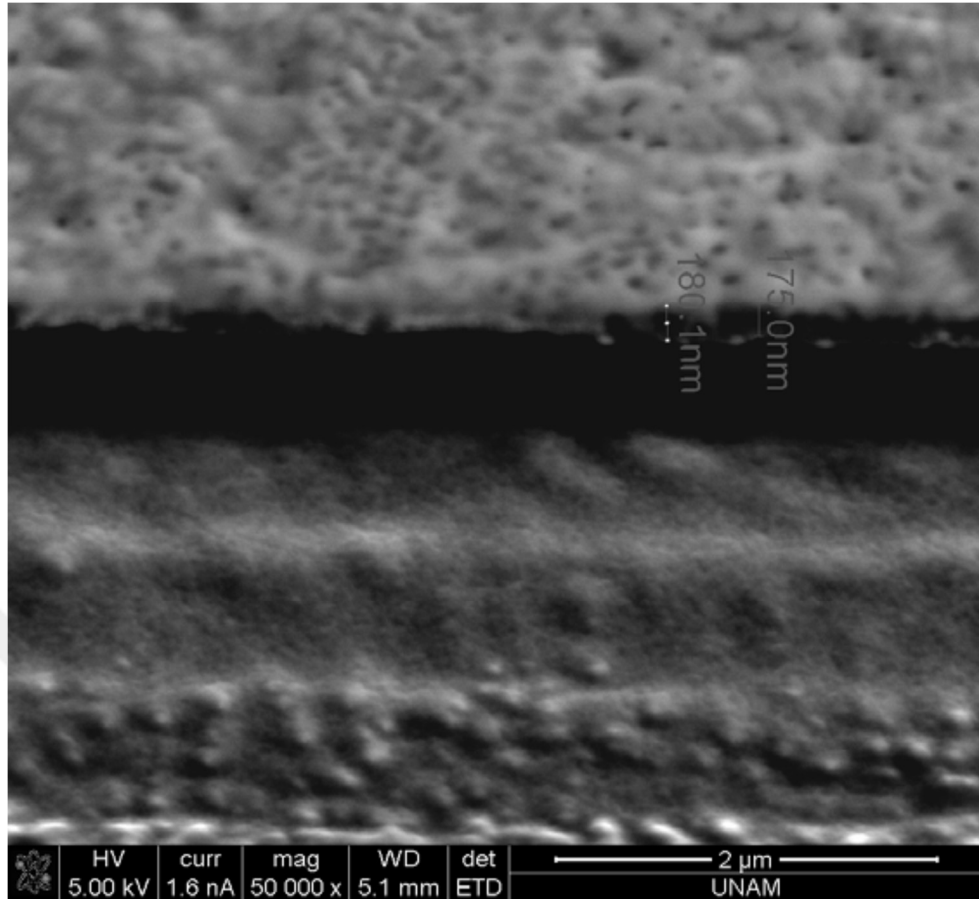
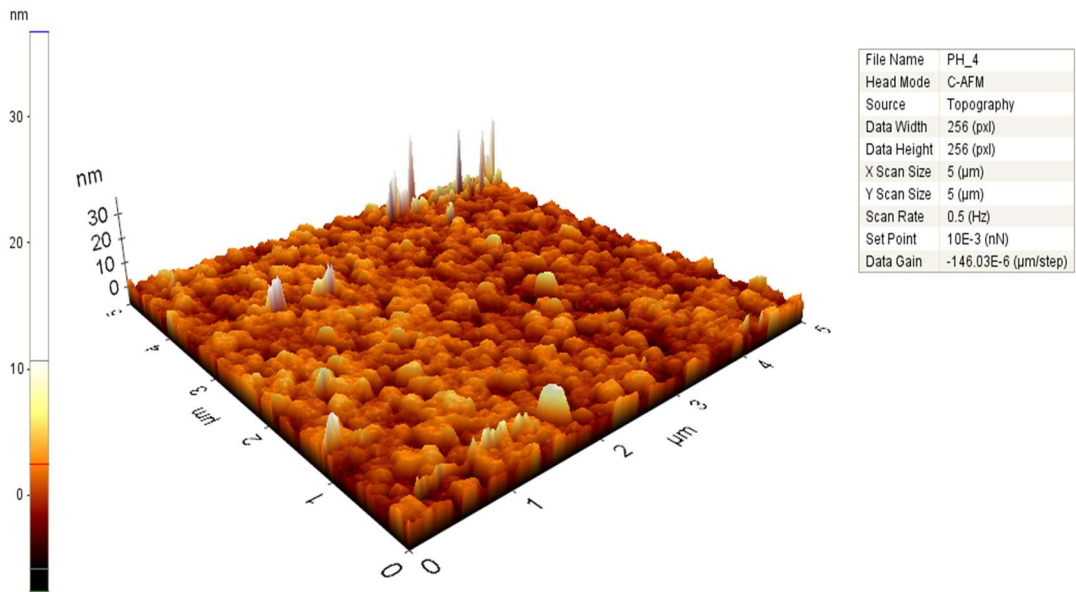
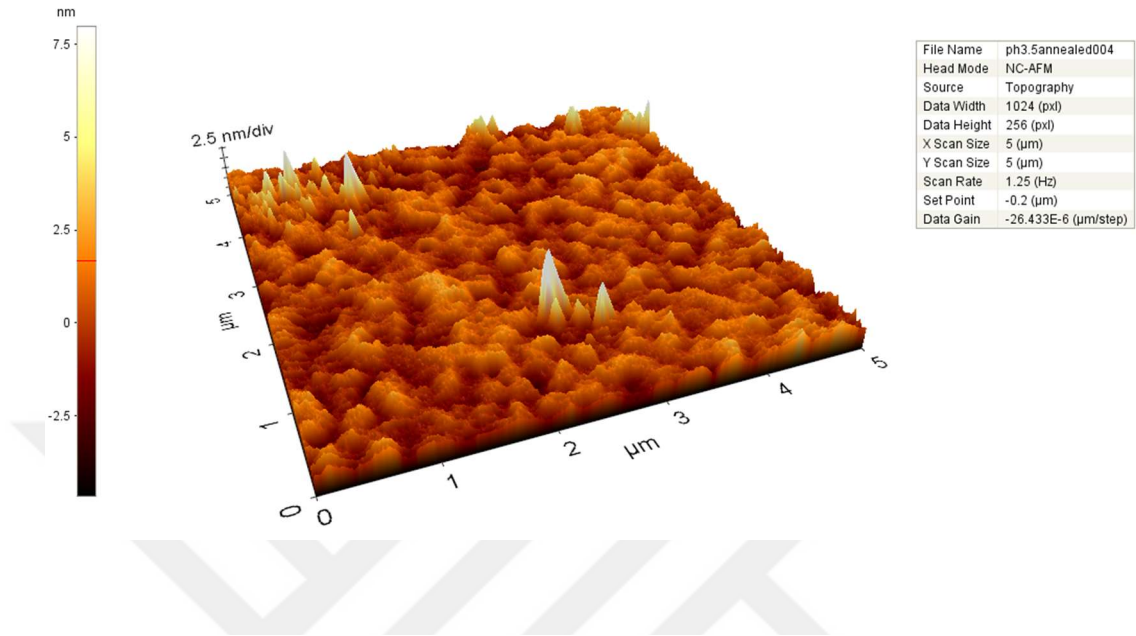


**Figure 3.5** Thickness measurements with SEM [59].

Film thickness was measured by ionically etching the coated film. As it is seen from Figure 3.5, coated surface of the film was etched ionically by focused ion beam (FIB) then tilted  $53^\circ$  in the vacuum chamber of the SEM. It can be seen from the image, which is taken from the etched and tilted surface, that film thickness about 120 nm. The examined film was coated by dipping two times so the film thickness for each dip can be said as 60-70 nm [59].

### 3.3 Surface Morphologies of Films

#### 3.3.1 Atomic Force Microscopy (AFM)



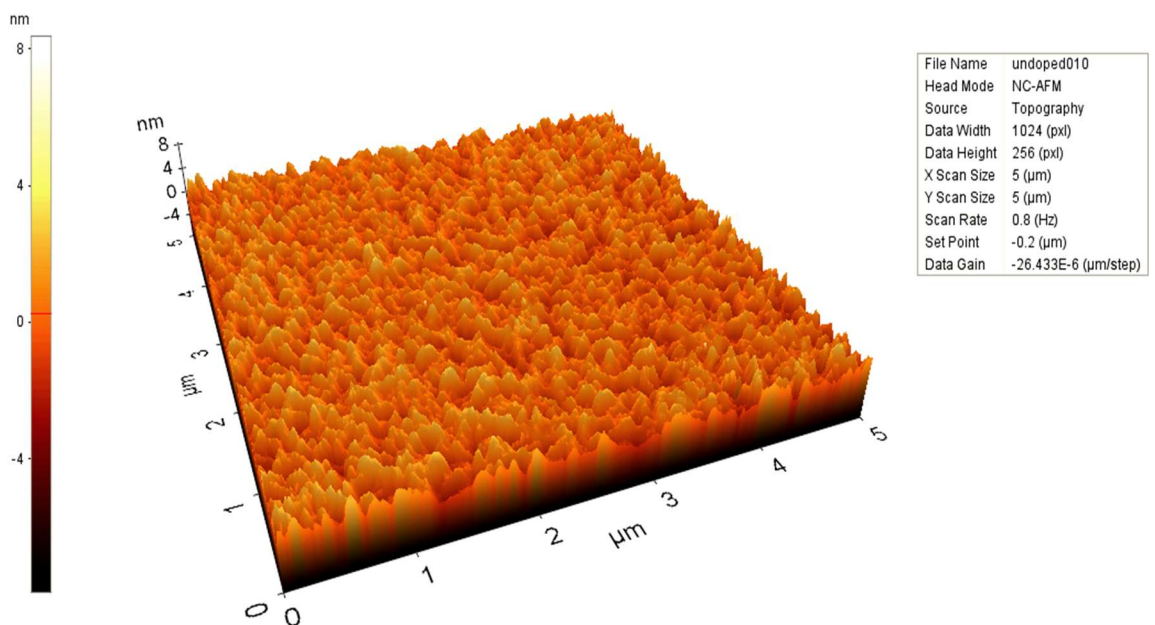
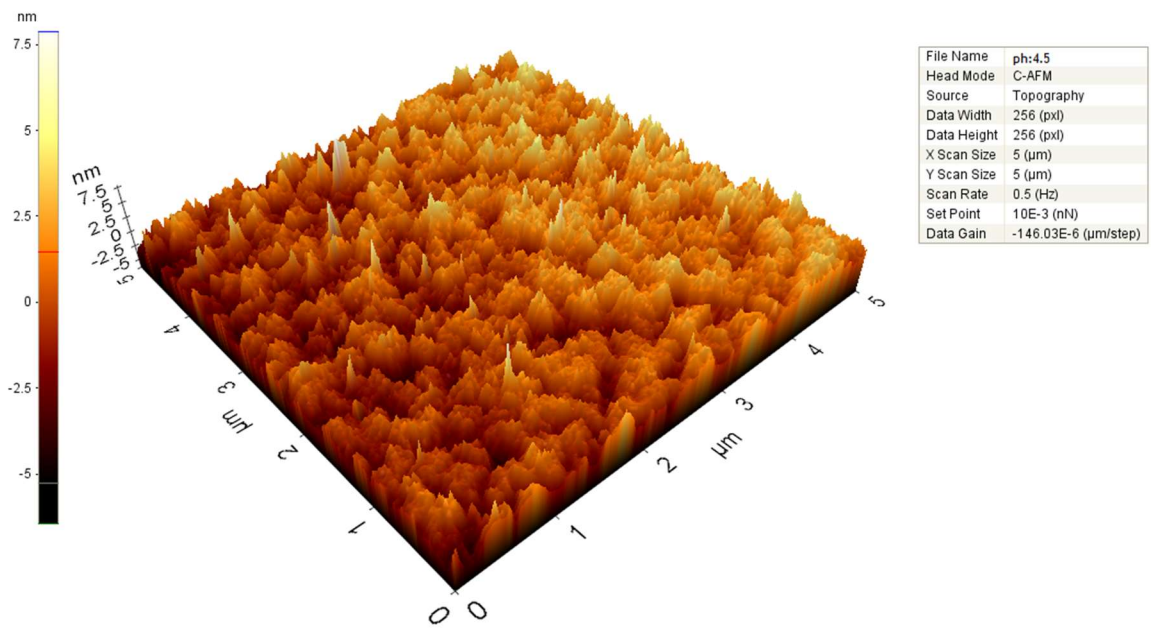


**Figure 3.6** AFM XEI program profilometer images the samples of A1, A2, A3, and A4

Surface examination was performed with atomic force microscopy (AFM). Coated surfaces are detected and pH effects on surface modification of thin films were investigated. 5-5μm of surface is scanned and the output images are saved. According to scanning results pH factor is very important factor on film morphology. Different pH values caused different surface morphology. The images of AFM

results are given above. They show that surface properties and structures of grains vary with different pH values. Previous research shows that the pH change of sol is directly affect the grain morphology [60].

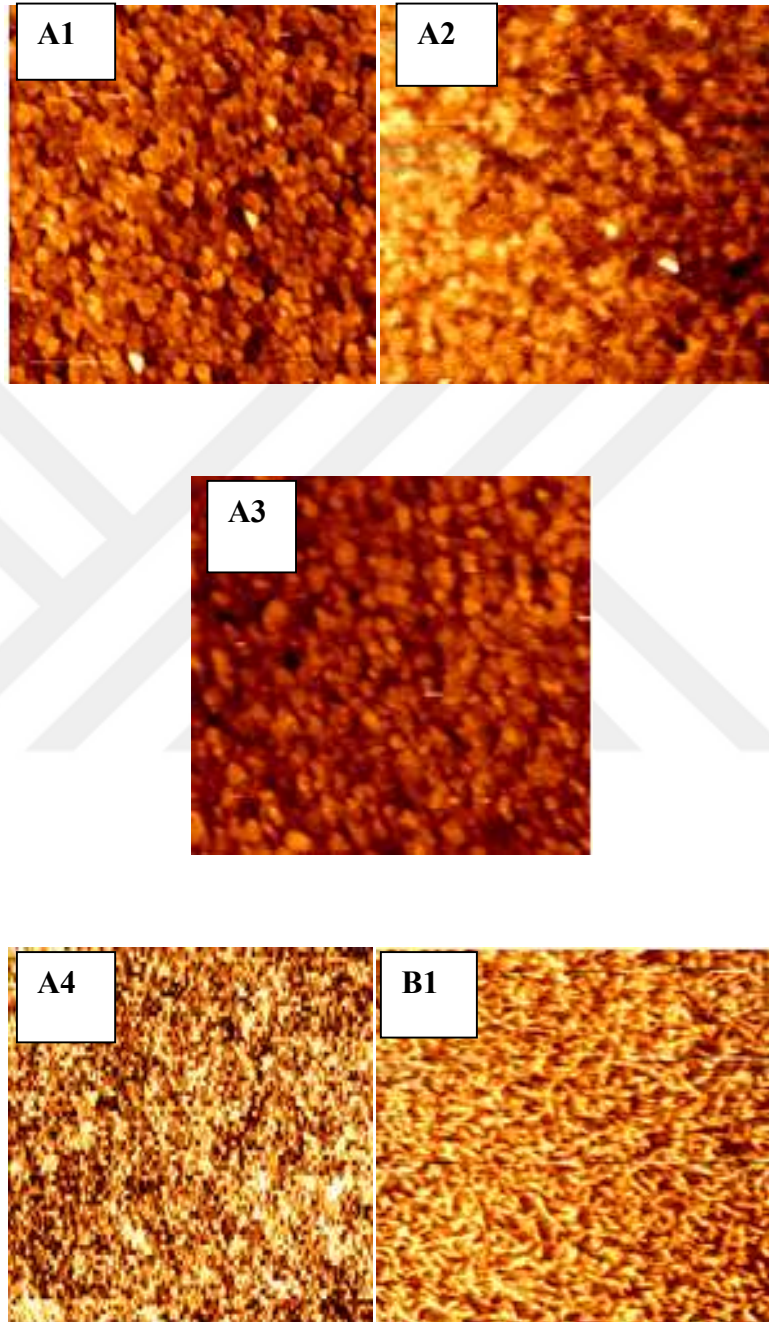


**Figure 3.7**AFM images of TiO<sub>2</sub> samples with different pH. (A1, A2, A3, A4 and B1)

The images show the ph effect on surface morphology. Increasing pH brings increasing in average surface area. Low pH values caused small grain structure and

the boundaries are more prominent and they can be seen very clearly in the profilometer results. Structure of thin film surface is small and the boundaries can be seen clearly.

This profilometer images obtained from AFM XEI program. The results are given in tiff format from the XEI program. The profilometer images to be obtained from AFM were characterized with the program, Gwyddion-2.36.win32.pro. This program make possible to examine the images from different angles. By using Gwyddion-2.36.win32.pro, average height of the grains in the structure of the thin film is calculated approximately.

From all of these calculations, it is clearly seen that pH change is a key effect on surface morphology of tin film. A graph below, the ph values versus average roughness values shows the ph effect on average roughness parameters. As can be seen in the graph roughness values are increasing linearly with the increasing pH.

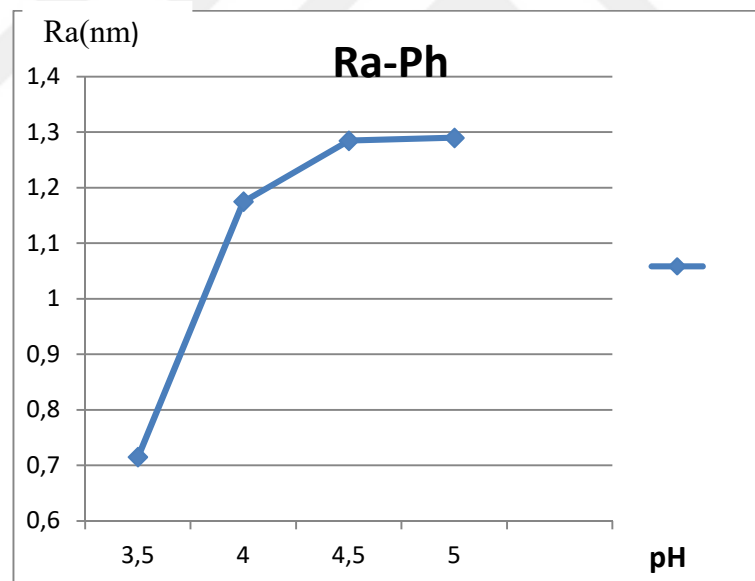


**Figure 3.8** Average roughness versus pH

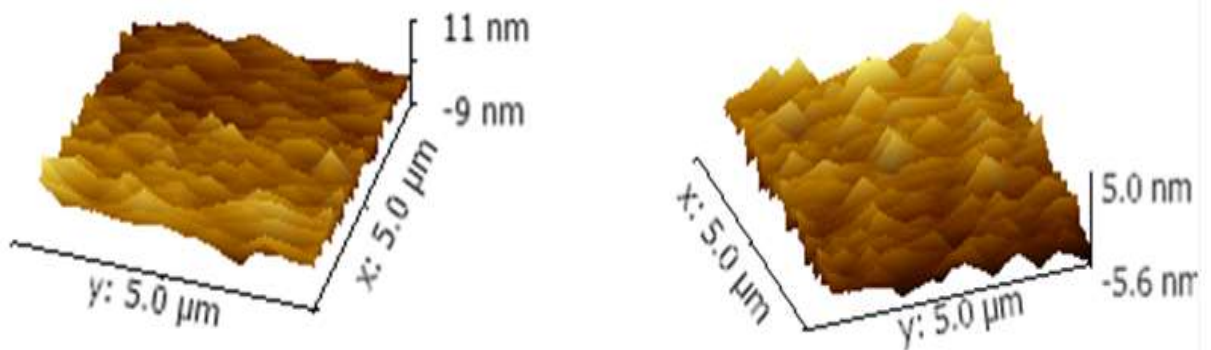
Our pH values of sols are all in acidic range so the pH values are quite low. Due to the low pH values, the grain structure of thin film surface is small and the boundaries can be seen clearly. Working pH range is fairly narrow. The difference between each pH values is 0.5. so roughness values of each samples are very close to one

another(each other). Low pH values caused smaller and specific grain structure. Small and specific grain structure provides the increasing of surface area. Increase in the surface roughness is to increase the surface area. (Figure 1.8) By using this property an increase of the efficiency of thin films used in solar cells could be succeeded.

**Table 4.**Effect of pH on surface Ra values of samples (Gwyddion-2.36.win32.pro)

Precursor	pH	Code	Ra (nm) (average roughness)
Titanium Methoxide	Ph =4,0	A1	1,175
Titanium Methoxide	Ph =4,5	A2	1,285
Titanium Methoxide	Ph =5,0	A3	1,290
Titanium Methoxide	Ph =3,5	A4	0,715
Titanium Butoxide	Ph =4,5	B1	1.27

Different solutions are prepared by using different precursors for investigation the precursor effect on film roughness parameter. It is clearly seen in Table 4 that, the precursor material also has an effect on film morphology. Roughness results are calculated and so the precursor effects can be analyzed. It is possible to say that the methoxide on at the same pH increased the roughness value of sample surface.



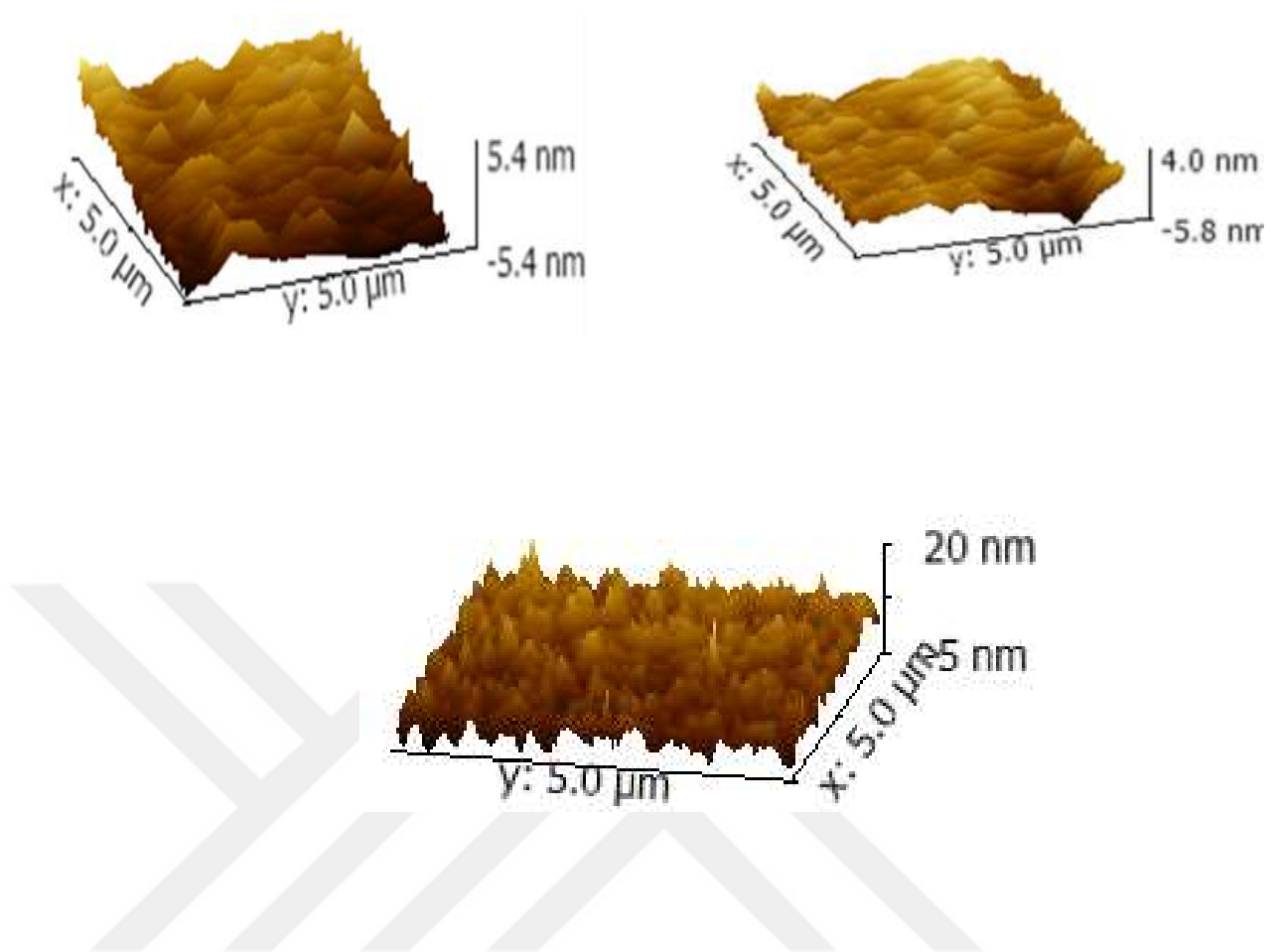


**Figure 3.** 3D AFM images of samples (A1, A2, A3, A4, and B1) (Gwyddion-2.36.win32.pro)



# CHAPTER 4

## CONCLUSION AND RECOMMENDATIONS

### 4.1 Conclusion

Experimental results show that,

1. Coating and formation of  $\text{TiO}_2$  observed successfully on ITO substrates.
2. The thickness of tin films is about 60 nm for per dipping.
3. pH effect on film surface is investigated intensively.
4. It can be said that one more time, for homogeny coating and formation of thin film on the surface sample can be occurred the pH ranges must be in acidic limits.
5. Increasing pH caused to increase in roughness values of film surface. Also it is clearly observed that the roughness of surface value is a pH dependent factor.
6. Used precursor, is also effective on the surface properties of tin films. By means of precursor affect, the roughness parameter of titanium methoxide is higher than the roughness parameter of titanium butoxide.
7.  $\text{TiO}_2$  were formed noticeably but the crystallization process and transformation of anatase to rutil has not been occurred since the operating temperature is lower than the phase formation temperature

### 4.2 Recommendations

Several recommendations for the future researches are listed as below.

1. Besides the pH effect, the annealing time effect can be measured with different holding times.
2. Annealing temperature could be increased with this way phase transformation of  $\text{TiO}_2$  will be occurred.
3. Samples could be annealed with different temperatures that the temperature effect can be determined.

4. Ph ranges of sols can be changes. In acidic and basic sols are prepared and with same conditions substrates will be coated and effect of the acidic and base sols could be measured.
5. As a precursor material very different materials could be used and according to solubility properties thickness and the roughness parameters can be evaluated.



# REFERENCES

- [1] Smestad G., 'Titanium Dioxide Solar Cell' Adapted by Lauren Cassidy and Thomas. C. Keane, Ph.D., 2010, Institute for Chemical Education, Madison WI
- [2] Aohan Y., 2011, 'Coating, Titanium Dioxide and Solar Cell', Saimaa University of Applied Sciences, Imatra Technology, Degree Programme in Paper Technology Bachelor's Thesis,
- [3] The Real Lifespan of Solar Panels". Energy Informative. The Homeowner's Guide to Solar Panels, 7 May 2014.
- [4] W. H. Bloss, F. Pfisterer, M. B. Schubert, and T. Walter 'Thin Film Solar Cells Invited review', 1995, 10.1002/pip.4670030102
- [5] K.L Chopra, P.D. Paulson and V.Dutta., 'Progress in Photovoltaic's, Research and Applications, Thin Film Solar Cells- An Overview' 12,69-92,2004
- [6] Dorian A.H. Hanaor , Charles C. Sorrell (February 2011) *Review of the anatase to rutil phase transformation*, DOI 10.1007/s10853-010-5113-0
- [7] Gratzel, M., (2003). 'Dye-sensitized solar cells.' *Journal of Photochemistry and Photobiology C: Photochemistry Reviews* 4, pp. 145–153
- [8] Zhu, K.; Neale, N.R.; Halverson, A.F.; Kim, J.Y. & Frank, A.J. (2010). 'Effects of Annealing Temperature on the Charge-Collection and Light-Harvesting Properties of TiO<sub>2</sub> Nanotube-Based Dye-Sensitized Solar Cells.' *J. Phys. Chem. C*, Vol. 114 (32), pp 13433–13441.
- [9] O'Regan, B.; Grätzel, M., 'A Low-Cost, High Efficiency Solar Cell Based on Dye-Sensitized TiO<sub>2</sub> Colloidal Films *Nature*' 1991, 353, 737– 740
- [10] A.R. Zainun, S. Tomoya, U.M. Noor, M. Rusop, I. Masaya, 'New approach for generating Cu<sub>2</sub>O/TiO<sub>2</sub> composite films for solar cell applications', *Mat. Lett.*, 66, 1, pp. 254-256, 2012
- [11] Y.Li,J. Heagen, W.Schafrath,P. Otschik, D. Haarer, 'Titanium Dioxide Films for Photovoltaic Cells Derived From Sol-Gel Process', *Sol. Energy. Sol. Cells* 56, 1999, 167-174
- [12] Andrea C, Zerulla D., 'Optimisation of Ruthenium Dye Sensitised Solar Cells Efficiency via Sn Diffusion into the TiO<sub>2</sub> Mesoporous Layer' 2013 May 21. doi: 10.1371/journal.pone.0063923

- [13] R. Advincula and W. Knoll., '*Functional Polymer Films*' Eds– Wiley, 2011, ISBN 978-3527321902.
- [14] Dr. A. Bergauner, Dr.C.Eisenmenger '*Thin Film Technology/Physics of Thin Films*' Chapter 4 LVA nr. 138.030,138.032
- [15] C. J. Brinker and G. W. Sherer, '*Sol-Gel Science*', Academic Press, San Diego, 1990
- [16] C. J. Brinker, A. J. Hurd, P. R. Schunk, C. S. Ashely, R. A. Cairncross, J. Samuel, K. S. Chen, C. Scotto and R. A. Schwartz, '*Sol-Gel Derived Ceramic Films--Fundamentals and Applications*', in: K. Stern (Ed.), Metallurgical and Ceramic Protective Coatings, Chapman & Hall, London, 1996, pp. 112-151.
- [17] T. Troczynski and Q. Yang, "*Process for Making Chemically Bonded Sol-Gel Ceramics*". U.S. Pat. No. 6,284,682, May, 2001.
- [18] T. Olding, M. Sayer and D. Barrow, '*Ceramic Sol-Gel Composite Coatings for Electrical Insulation*', Thin Solid Films 398-399 (2001) 581-586.
- [19] C. Jeffrey Brinker (Author),George W. Scherer , *Sol-Gel Science: The Physics and Chemistry of Sol-Gel Processing*, Academic Press, Inc
- [20] S.M. Atia, Wang J., Guanming WU, Shen J, Jianhua MA., '*Review on Sol-Gel Derived Coatings: Process, Techniques and Optical Applications*', April16,2001-July,16,2001
- [21] Perednis, D. '*Thin Film Deposition by Spray Pyrolysis and the Application in Solid Oxide Fuel Cells*', Thesis (PhD), Swiss Federal Institute of Technology Zurich, 2003
- [22] D. Depla , S. Mahieu , J.E. Greene, '*Sputter Deposition Processes*',Ghent University, Department of Solid State Sciences, Krijgslaan 281 (S1), 9000 Ghent, Belgium, Materials Science and Physics Departments and the Frederick Seitz Materials Research Laboratory, University of Illinois, Urbana, Illinois 61801, USA.2009
- [23] Nalwa, H.,S, '*Nanomaterials and magnetic thin films* ',Handbook of thin film materials Volume 5,2002
- [24] Goyal,A. '*Methodsof HTS Deposition: Thermal Evaporation*' In book: Second-Generation HTS Conductors, pp.81-96,2005

- [25] Bo Cui, '*NE 343: Microfabrication and thin film technology*', University of Waterloo, 2000
- [26] NE 343: Microfabrication and thin film technology Instructor: Bo Cui, ECE, University of Waterloo; Textbook: Silicon VLSI Technology by Plummer, Deal and Griffin
- [27] Zhou M, Roualdès S, Zhao J, Autès V, Ayrál A. '*Nanocrystalline TiO<sub>2</sub> thin film prepared by low-temperature plasma enhanced chemical vapor deposition for photo catalytic applications*' Thin Solid Films, vol. 589, pp. 770-777, 2015
- [28] Oka N, Sanno Y, Jia J., Nakamura S., Shigesto Y. '*Transparent Conductive Nb-Doped TiO<sub>2</sub> Films Deposited By Reactive Dc Sputtering Using Ti-Nb Alloy Target, Precisely Controlled In The Transition Region Using Impedance Feedback System*', 2011
- [29] F.Z.Bedia, A.Bedia, N.Maloufi, M.Aillerie, F.Genty, B.Benyoucef, '*Effect of tin doping on optical properties of nanostructured ZnO thin films grown by spray pyrolysis technique*' Journal of Alloys and Compounds, 2014
- [30] E.Mokaripoor, M.-M.Bagheri-Mohagheghi '*Study of structural, electrical and photo conductive properties of F and P co-doped SnO<sub>2</sub> transparent semiconducting thin film deposited by spray pyrolysis*' , Materials Science in Semiconductor Processing, 2015
- [31] Senain I., Nayan N., Saim H. '*Structural and Electrical Properties of TiO<sub>2</sub> Thin Film Derived from Sol-gel Method using Titanium (IV) Butoxide*' International Journal of Integrated Engineering (Issue on Electrical and Electronic Engineering)
- [32] Siti Aida Ibrahim, and Srimala Sreekantan, '*Effect of pH on TiO<sub>2</sub> nanoparticles via sol gel method*' International Conference on X-Rays & Related Techniques in Research & Industry, 2010
- [33] Young S. K., '*Overview of Sol-Gel Science and Technology*', Army Research Laboratory, 2002
- [34] K Sivakumar, V Senthil Kumar, N Muthukumarasamy, M Thambidurai, TS Senthil, '*Influence of pH on ZnO nanocrystalline thin films prepared by sol-gel dip coating method*' , Bulletin of Materials Science, 2012

- [35] H.SamariJahromi, H.Taghdisian, S.Afshar, S.Tasharrofi., ‘*Effects of pH and polyethylene glycol on surface morphology of TiO<sub>2</sub> thin film*’,2009
- [36] A. Kassim, W. T. Tan, S. M. Ho, N. Saravanan. ‘*Influence Of Ph On The Structural And Morphological Properties Of ZnS Thin Films*’, AnadoluÜniversitesiBilimveTeknolojiDergisi A - UygulamalıBilimlerveMühendislik , Cilt.11 Sayı.1 , 2010 24
- [37] Abbas N. M., Kunieda M., ‘*Micro-EDM with Controlled Pulse Train Method using Small Feeding Capacitance*’ 18th CIRP Conference on Electro Physical and Chemical Machining (ISEM XVIII)
- [38] Pokaipisit A., Horprathum M., Limsuwan P. ‘*Influence of Oxygen Flow Rate on Properties of Indium Tin Oxide Thin Films Prepared by Ion-Assisted Electron Beam Evaporation*’ Songklanakarin J. Sci. Technol.31 (5), 577-581, Sep. - Oct. 2009
- [39] Indium corporation; Indium Tin Oxide (ITO), product data sheet. <http://www.indium.com/inorganic-compounds/indium-compounds/indium-tin-oxide/07.06.2016>
- [40] Sigma-Aldrich, 703192 ALDRICH Indium tin oxide coated glass slide <http://www.sigmaaldrich.com/catalog/product/aldrich/703192?lang=en&region=TR07.06.2016>
- [41] Çörekçi S. Ph. D. Thesis. ‘*AFM Surface Characterization in Group III-V Compound Semiconductors*’ Gazi University Institute of Science and Technology, January 2008
- [42] Bhushan B., Marti O., ‘*Scanning Probe Microscopy – Principle of Operation, Instrumentation, and Probes*’ ,DOI 10.1007/978-3-642-15283-2\_2, Springer-Verlag Berlin Heidelberg 2011
- [43] Park Systems How AFM Works <http://www.parkafm.com/index.php/medias/nano-academy/how-afm-works> 07.06.2016
- [44] G Rijnders, G Koster ‘*In Situ Characterization of Thin Film Growth*’,October 2011,ISBN: 9781845699345

- [45] Zhuang L, Bao S, Wang R, Li S, Ma L, DechunLv ‘*Thin Film Thickness Measurement Using Electron Probe Microanalyzer*’ Proceedings of 2009 IEEE International Conference on Applied Superconductivity and Electromagnetic Devices Chengdu, China, September 25-27, 2009
- [46] Dr. A. Bergauner, Dr.C.Eisenmenger ‘*Thin Film Technology/Physics of Thin Films*’ Chapter 4 LVA nr. 138.030,138.032
- [47] Maniscalco B, Kaminski M., Walls J M. ‘*Combined Thin-Film Thickness Measurement and Surface Metrology of Photo voltaic Thin Films Using Coherence Correlation Interferometry*’ 978-1-4673-0066-7/2011 IEEE
- [48] Mladenova D., Siderov V., Zhivkov I., Salyk O., Ohlídal M., Yordanova I., Yordanov R., Philippov P., Weiter M ‘*Thin Film Technology/Physics of Thin Films*’ Chapter 4 LVA nr. 138.030,138.032)
- [49] L. R. Cruz, C. L. Ferreira and D. T. Gomes ‘*Thin Film Thickness Measurement Using The Energy dispersive Spectroscopy Technique In A Scanning Electron Microscope*’ Thin Solid Films, 185 (1990) 279-286 Preparation and Characterization)
- [50] Göller K. ‘*Spectroscopic ellipsometry study on the oxide films formed on nickel-base alloys in simulated boiling water reactor environments*’ ISRN UTH-INGUTB-EX- KKI-2011/01-SE Examensarbete 15 hpJuni 2011
- [51] Cao C., Chan H. F., Zang J., Kam W., and Zhao X. ‘*Harnessing Localized Ridges for High-Aspect-Ratio Hierarchical Patterns with Dynamic Tunability and Multifunctionality*’ for Adv. Mater., DOI: 10.1002/adma. 201304589
- [52] Hitachi High-Tech Science Corporation RBM Tsukkjii Bldg., 15-5, Shintomi 2-chome, Chuo-ku, Tokyo 104-0041 Application Brief 2009.4)
- [53] Sezen H., ‘*Photo-Dynamic XPS for Investigating Photoinduced Voltage Changes in Semiconducting Materials*’, P.h. D. Thesis, Engineering and Science of Bilkent University, December, 2011
- [54] Sezen H., ‘*Investigation on Electrical Charging/Discharging Properties of Thin PS/PMMA Polymeric Films by Dynamic X-Ray Photoelectron Spectroscopy*’ M.Sc. THESIS, Engineering and Science of Bilkent University, May 2008
- [55] Loye H. Z., ‘X-Ray Diffraction How It Works’, University of South Caroline Bicentennial

- [56] DEMİREZEN B., '*Examination of Polymeric Azomethine Compounds and Transition Metal Complexes by Using XRD and XRF*', M.Sc. THESIS, University of Kahramanmaraş Sutcu Imam, Department of Physics, December/2014
- [57] Geochemical Instrumentation and Analysis, How does it work, online doc. [http://serc.carleton.edu/research\\_education/geochemsheets/techniques/XRD.htm](http://serc.carleton.edu/research_education/geochemsheets/techniques/XRD.htm)  
108.06.2016
- [58] Jolm F. Moulder William F. Stickle Peter E.'SobolKennetlf D. BombenHandbook of X-ray Photoelectron SpectroscopyReference Book of Standard Spectra for Identification and Interpretation of XPS Data,Reference Book of Standard Spectra for Identification and Interpretation of XPS Data
- [59] OKUYUCU H., KONAK T., ÇİNİCİ H., '*Coating of Nano Sized Ionically Conductive Films by Sol-Gel Route*'Gazi University, Faculty of Technical Education, ANKARA TURKEY
- [60] SamariJahromia H. , Taghdisiana H, Afshar S., Tasharrofi S., '*Effects of pH and polyethylene glycol on surface morphology of TiO<sub>2</sub> thin film*'doi:10.1016/j.surfcoat.2009.01.034



# RESUME(CV)

## PERSONAL INFORMATION

**Name Surname** :Güldane ERTUĞRUL  
**Date of Birth** :29.09.1988  
**Phone** :554 293 75 56  
**E-mail** :guldaneertugrul@karabuk.edu.tr

## EDUCATION

**High School** :Karabük Anatolian High School / KARABÜK (2003-2007)  
(80/100)  
**Bachelor** :19 Mayıs University / SAMSUN (2008-2012)  
(3.16/4.0)  
**Master Degree** :Ankara Yıldırım Beyazıt University (2012-continued)

## PROFESSIONAL EXPERIENCE

**Research Asst.** :University of Karabük (2016-continued)

## TOPICS OF INTERESTS

-Thin Film Coating  
-Thin Film Surface Characterization Methods